

University of Louisville
ThinkIR: The University of Louisville's Institutional Repository


Electronic Theses and Dissertations

5-2019

The Q rule in Bacteriodes and the identification and characterization of Porphyromonas gingivalis Glutaminyl Cyclase.

John Andrew Houston
University of Louisville

Follow this and additional works at: <https://ir.library.louisville.edu/etd>

 Part of the [Bacteriology Commons](#), [Biochemistry, Biophysics, and Structural Biology Commons](#), and the [Oral Biology and Oral Pathology Commons](#)

Recommended Citation

Houston, John Andrew, "The Q rule in Bacteriodes and the identification and characterization of Porphyromonas gingivalis Glutaminyl Cyclase." (2019). *Electronic Theses and Dissertations*. Paper 3201.
<https://doi.org/10.18297/etd/3201>

This Doctoral Dissertation is brought to you for free and open access by ThinkIR: The University of Louisville's Institutional Repository. It has been accepted for inclusion in Electronic Theses and Dissertations by an authorized administrator of ThinkIR: The University of Louisville's Institutional Repository. This title appears here courtesy of the author, who has retained all other copyrights. For more information, please contact thinkir@louisville.edu.

THE Q RULE IN *BACTERIODETES* AND THE IDENTIFICATION AND
CHARACTERIZATION OF *PORPHYROMONAS GINGIVALIS* GLUTAMINYL
CYCLASE

By

John Andrew Houston

B.S. Samford University

DMD University of Louisville

A Dissertation

Submitted to the faculty of the

Graduate School

In Partial Fulfillment of the Requirements

For the degree of

Doctor of Philosophy in Interdisciplinary Studies

Interdisciplinary Studies

University of Louisville

May 2019

THE Q RULE IN *BACTERIODETES* AND THE IDENTIFICATION AND
CHARACTERIZATION OF *PORPHYROMONAS GINGIVALIS* GLUTAMINYL
CYCLASE

John Andrew Houston

B.S. Samford University

DMD University of Louisville

A Dissertation Approved on

November 30th, 2018

By the Dissertation Committee:

Director: Dr. Jan Potempa

Dr. Richard Lamont

Dr. James Graham

Dr. Don Demuth

Dr. David Scott

DEDICATION

This dissertation is dedicated to my parents, Jimmy Allen Houston and Melinda Harris Houston, who have given me unlimited educational potential and the drive to succeed and most importantly my wife, Emily Meadows Houston who has given me endless support and boundless encouragement to continue my passion.

ACKNOWLEDGEMENTS

I would like to especially thank my mentor Dr. Jan Potempa for his unwavering support and endless patience. Without your teaching and assistance none of this body of work could have ever been possible. I would also like to thank the members of my committee: Dr. Richard Lamont, Dr. David Scott, Dr. Don Demuth, and Dr. James Graham for their support and help these past seven years. I would like to also acknowledge the faculty and administration of the University of Louisville School of Dentistry for making this dual degree program a reality and facilitating its integration with my clinical coursework. It has been a journey fraught with peril but yet we emerge relatively unscathed. I would like to thank the many members of Dr. Potempa's lab, who have taught me so much. Lastly, I would like to acknowledge my wife Emily, who has stood by me through the long nights, early mornings, and stressful days with open arms and warm smiles. This work is for you.

ABSTRACT

THE Q RULE IN *BACTERIOIDES* AND THE IDENTIFICATION AND CHARACTERIZATION OF *PORPHYROMONAS GINGIVALIS* GLUTAMINYL CYCLASE

John Andrew Houston

November 30th, 2018

Background: *Porphyromonas gingivalis*, a major pathogen associated with chronic periodontitis, secretes variety of proteins, majority of which begins with glutamine. Several of these proteins were found with pyroglutamate (pGlu) at N-terminus suggesting the presence of this posttranslational modification pathway in *P.gingivalis*. The observation that N-terminal glutamine is over-represented as the first amino acid after signal peptide cleavage, and subsequent confirmation of pGlu formation on the nascent protein via mass spectrometry, led us to conclude that an enzyme must be present as the executor of this reaction. Hypothesis: PG2157 is a glutaminy cyclase and is responsible for the cyclization of N-terminal glutamine residues. Methods: A homology search was used to identify a gene (*PG2157*) encoding a protein homologous to human glutaminy cyclase (QC) in the *P. gingivalis* genome. The gene was cloned, expressed in *E. coli* and recombinant PgQC purified. The protein was crystalized, and structure determined by molecular

replacement. The rPgQC activity was characterized with respect to pH, ionic strength, optimum substrate specificity, and sensitivity to inhibition by an array of non-specific and specific inhibitors. Finally, subcellular localization of PgQC in *P. gingivalis* was determined. Results: PgQC specificity is restricted for N-terminal glutamine. The enzyme converts this residue to pGlu with k_{cat}/K_m at 1.34 s^{-1} . The reaction was fastest at low ionic strength and at pH around 8.0. The activity was inhibited by *o*-phenanthroline ($\geq 100 \mu\text{M}$) and EDTA ($\geq 100 \text{ mM}$ EDTA). Cu^{2+} and Zn^{2+} at $\geq 100 \text{ nM}$ exerted $\geq 90\%$ inhibition. The activity was also significantly affected by cysteamine, imidazole, and reduced glutathione. In bacterial cells PgQC was found associated with the inner membrane as a lipoprotein facing the periplasm. The crystalline structure of PgQC showed strong similarity to human QC on the atomic level. Nevertheless, an inhibitor specific for human QC had a limited effect on the PgQC activity. Conclusions: PgQC is an enzyme resembling mammalian QC and it is responsible for pyroglutamination of proteins secreted by the T9SS of *P. gingivalis*. This activity is likely essential for bacterium viability since all attempts to produce a viable PgQC knockout failed. Taking into account that also *T. forsythia* and *P. intermedia* possess similar enzymes and the frequency of the Q value of *Bacteroidetes* it is likely that similar post-translational modification plays a pivotal role in protein secretion by these periodontal pathogens. Therefore, inhibition of bacterial QC may represent a novel approach to treat periodontal diseases.

TABLE OF CONTENTS

	PAGE
DEDICATION	iii
ACKNOWLEDGMENTS	iv
ABSTRACT.....	v
LIST OF TABLES	ix
LIST OF FIGURES	x
INTRODUCTION.....	1
HYPOTHESIS.....	26
SPECIFIC AIMS.....	25
METHODS AND MATERIALS	27
Cloning, Expression, and Purification of recombinant PgQC.....	27
<i>P. gingivalis</i> QC Activity Assay.....	28
<i>P. gingivalis</i> Culture and Cell Fractionation.....	29
<i>P. gingivalis</i> Δ RgpB Deletion Mutant.....	30
Generation of Pg Mutant Strains.....	33
Gingipain Activity Assay.....	36

In vivo QC Specific Inhibitors.....	37
Affinity Purified anti-QC Antibodies.....	38
SDS-PAGE and Western Blotting.....	41
RESULTS & DISCUSSION	44
REFERENCES	84
CURRICULUM VITA.....	92

LIST OF TABLES

TABLE	PAGE
1. Periodontal Diseases in Humans.....	3
2. Primers for <i>P. gingivalis</i> Mutagenesis.....	34
3. CELLO Predictions.....	45
4. rPgQC Enzyme Kinetics.....	48
5. Attenuation of rPgQC Activity by Reducing Agents and Imidazole.....	52
6. rPgQC Activity in the Presence of Competing Metal Ions.....	55
7. Q-values for <i>P. gingivalis</i> and <i>T. forsythia</i>	58

LIST OF FIGURES

FIGURE	PAGE
1. N-terminal Cyclization of Glutaminyl Peptides by QC.....	18
2. Acceleration of Glutaminyl Cyclization by Ions.....	21
3. <i>P. gingivalis</i> Mutant Strains.....	34
4. Specificity of anti-QC Antibodies.....	38
5. Q-value Distribution in <i>Porphyromonas</i>	44
6. Purification of rPgQC.....	47
7. PgQC is an Inner Membrane Protein.....	50
8. Inhibition by 1,10-phenantroline and EDTA.....	53
9. Effect of Salt Concentration on rPgQC activity.....	54
10. Q Downstream of SPI Affects RgpA, not RgpB or Kgp.....	61
11. Structural Schematic of <i>P. gingivalis</i> Operon Containing QC.....	63
12. LL29 Inhibits <i>P. gingivalis</i> Growth.....	65
13. PgQC in vivo inhibition by LL29.....	66
14. 24-Hr Growth Inhibition of <i>P. gingivalis</i> W83.....	68
15. Q-value Averages and Q-value Distributions for Bacterial Groups.....	71
16. Sequence Downstream of Q in <i>T. forsythia</i> SPI Proteins.....	77
17. QC Activity in <i>T. forsythia</i>	78
18. LL29 Does Not Inhibit <i>T. forsythia</i> QC.....	79
19. Hypothesized Pathway for Pyroglutamate formation by QC.....	82

CHAPTER I: INTRODUCTION

Periodontal Disease

A periodontal diagnosis is a term that serves as a crucial determination of a patient's dental treatment outcome. Clinicians assign these diagnoses on patients as a culmination of the sum of all the clinical information, pertinent medical history, and dental history along with the gross findings from a completed periodontal and oral examination. All the clinical data along with the totality of signs and symptoms are aggregated together and with this sum of information the clinician may arrive at a diagnosis. Additionally, sometimes in more complicated cases, additional lab tests or supplemental information can be instrumental in coming to the correct conclusion. As a clinician, treatment of plaque-induced periodontal diseases generally results in the resolution of the periodontal infection. Also, it is vital to understand that periodontal treatment generally changes the pretreatment diagnosis to a usually more favorable post-treatment diagnosis. To demonstrate, effective prophylactic treatment routinely converts mild, moderate, and severe plaque-induced gingivitis into a state of periodontal health, when stressed with adequate home care instructions. To further illustrate this point, successful treatment of plaque-induced periodontitis, when followed up at re-evaluation appointment, will often be converted to a state of periodontal health with reduced periodontium, indicating that treatment has achieved the goal of creating shallower pocket depth measurements.

Periodontal disease is term that encompasses multiple differential modalities into one general disease term. Within the diagnosis of periodontal disease, there are more diverse classification systems that both clinicians and researchers alike use. The most descriptive and thorough clinical classification system was described by Armitage in 1999, and is still utilized by clinicians today [1].

Table 1 Presentation of Periodontal Diseases in Humans

Chronic Periodontitis (localized/generalized)
Localized Aggressive Periodontitis (LAP)
Generalized Aggressive Periodontitis (GAP)
Periodontitis as a Manifestation of Systemic Disease Associated with Hematologic Disorders Associated with Genetic Disorders
Necrotizing Ulcerative Periodontitis
Combined Periodontic-Endodontic Lesions
Abscesses of the Periodontium

Armitage [1-3]

Most patients who present with plaque-induced periodontitis will in fact possess the chronic form of the disease [4-7]. The most likely presentation of a chronic periodontitis patient is a patient greater than 30 years of age; gross plaque and calculus, substantial gingival inflammation is present, deepened periodontal pockets (> 3mm), and the presence of calculated periodontal attachment loss. Generally speaking chronic periodontal disease is a slow continuously progressing disease[8-10], but within this process may exist short periods of advancing rapid attachment loss [11, 12]. Previously chronic periodontitis was given the misnomer “adult periodontitis” since only the adult population was believed to be susceptible to the disease. However, this has been shown to be false as a result of past and more recent epidemiologic data clearly showing that chronic periodontal disease can be present in younger populations [9, 13]. Although specifically chronic periodontitis can be observed to occur in either localized or generalized distributions within patients, these specific two forms appear to be vastly similar or almost identical with regards to their presentation, pathogenesis, and progression. Aggressive periodontitis, however, is far more rare than chronic periodontitis and mainly affects children and adolescents. It also can occur in both localized and generalized presentations, but unlike chronic periodontitis, these distributions differ significantly with respect to their pathogenesis [4, 13]. Localized aggressive periodontitis (LAP) and generalized aggressive periodontitis (GAP) were previously called “localized and generalized juvenile periodontitis”, respectively [14].

Biofilms

These different presentations of periodontal diseases are best described as multifactorial infections, which are elicited by the presence of an entire community of complex of bacterial species. This community of organisms referred to as a “biofilm” interacts with the host, specifically with connective tissue and immune cells, which in turn causes a release of large number of pro-inflammatory cytokines and chemokines. These pro-inflammatory mediators lead to the degradation and destruction of cellular structures of the periodontal organ, namely: bone, periodontal ligament, sulcular epithelium, and junction epithelium [15]. The trigger for the initiation of periodontal disease is the presence of dysbiotic microbial biofilms composed of bacteria that colonize the tooth surface in the sulcular region. This region lies between the tooth surface below the cement-enamel junction and the gingival margin and plaque formation is mediated through specific adherence interactions and accumulation due to architectural changes in the sulcus [16]. The characteristics of microbiological progression from periodontal health to gingivitis (e.g. chronic inflammation of the gingival tissue without tissue destruction), and eventually to periodontal disease are vast and complicated [17].

Although it has been previously estimated that out of nearly 1,000 different microbial taxa are able to colonize, at least transiently the oral cavity of humans and from a complex organized biofilm [18], it is still not fully understood how the

multitude of different species exist and work harmoniously to begin the pathogenic process and progress to full blown disease state. Previous studies have shown that of the just under 1000 species detected in the oral cavity approximately 500 are found to be present in periodontal plaque [19]. Some of these organisms most certainly are simply commensal or opportunistic species, but it is well documented that certain species drive the pathogenicity of the bacterial plaque into more virulent and destructive states [20]. Previous work has shown that even early colonizers and previously deemed commensals such as *Streptococcus gordonii* can have a profound effect on the pathogenicity of other organisms such as *A. actinomycetemcomitans* and *Porphyromonas gingivalis* [21]. It has been shown in several studies, and mentioned previously here that a multitude of bacterial species call the human mouth their home, humans overall understand very little about the consequences of harboring our bacterial inhabitants [22, 23]. Can the presence of just one of the “bad guys” turn our whole “neighborhood” into a difficult place to manage? Or does it take a combined effort of the community as a whole to corrupt our own host defenses. With regard to other dental diseases, such as dental caries, evidence is strong enough to allow us to point to the causative agent; *Streptococcus mutans* and *Lactobacillus sp.* Since these species have been identified, many papers have assessed the bacterial causative agents in patients in the varying states of periodontal health, gingivitis, and periodontitis [17, 20, 22, 24, 25]. We are aware of a great many gram-positive bacterial species that serves as beneficial commensal species and serve to help maintain important oral health. We now also know that as the progression of the disease proceeds and heads

further towards gingivitis and chronic periodontitis, greater numbers of gram-negative species begin to inhabit the sulcular epithelium and surrounding dentoalveolar structures. More striking though, is the simple fact that there is still no verifiable shown data, that one solitary species can solely cause the wide-ranging effects that periodontal disease can elicit in the mouth. No one organism can account for the varied destructive processes that occur in the disease process. This leaves us with the thought that the disease can only progress if several bacterial species join forces and the signs and symptoms of periodontal disease are in fact the result of a group effort. It must be clear then that a specific “consort” or “complex” of bacterial species must trigger the transition from a state of oral health to periodontal disease. Innumerable studies have focused on one specific bacterial species responsible for signs and symptoms of periodontal disease, but these do not account for the whole story. This, taken as a whole, supports the notion that the effects from periodontal disease must be the result of consortia of bacterial species acting as a complex biofilm to cause, elicit, and promote the disease [24-27]. Recently there has been reassessment of the “roles” of several bacterial species that are known to be involved in the progression of periodontal disease. These organisms were routinely found in examinations of patients who presented with periodontal disease and also in healthy controls. These species are now even commonly referred to as periodontopathogens. Included in this group are *P. gingivalis*, *A. actinomycetemcomitans*, *T. forsythia*, and *T. denticola*. Influential studies by Socransky and Haffajee [24] used newer methodology of stratifying these bacteria into their respective niches based on their roles within

oral microbiomes in the disease process leading to change from health to disease states. Researchers organized the organisms into groups or “complexes”. Individual complexes were based on the prevalence of the bacterial “affiliations” with one-another, and corresponding complexes associations with health, gingivitis, or periodontitis disease conditions [25-29]. These groups or complexes of different microbes were also stratified according to the sequence of colonization on the tooth surface in conjunction with periodontal disease severity. What Socransky et al. [20] labeled as the ‘red complex’ contained bacterial species that show up later in biofilm maturation phase. These bacterial species, namely, *P. gingivalis*, *T. denticola*, and *T. forsythia* (previous names *Bacteroides forsythus* or *Tannerella forsythensis*) were shown to be effective periodontopathogens [11, 20, 24, 26, 30]. In this same train of thought these investigators also concluded that this “red complex” represents the pinnacle of biofilm maturation and development and thus leading to advancing disease states.

Multiple other researchers have made note of this cooperation between species within the same complex and between members of different complexes. A strong association has been observed between *T. forsythia* and *P. gingivalis* found in periodontal pockets in patients, whilst in fact *P. gingivalis* has not been detected in the absence of *T. forsythia* within the periodontal pocket [31]. A strong relationship between *P. gingivalis* and *T. denticola* was found whilst taking plaque samples gathered in a study looking at diverse ethnic groups [32]. Moreover, constituent members of the red complex were located in significantly higher percentages in patients with periodontitis [33, 34] and also in probing sites with deeper pockets

[35-40]. These separate bodies of work support the theory that no one single bacterial species is etiologic for periodontal disease propagation or progression, and periodontal disease is not a singular “bacterial infection” but instead that the sum total of bacterial species in the oral cavity co-existing and co-habituating the oral microbiome are required to initiate the onset of periodontal disease. How these different species and organisms, as well as virulence determinants of the individual bacteria, contribute to disease progression remains unclear. Another hypothesis in more recent years has challenged the way we typically look at the “complexes” of oral microbiota in the mouth. While looking at the red complex organisms one would beg to ask the question, would higher numbers of these organisms correlate with greater periodontal tissue destruction. In fact, certain pathogens, more specifically, some from the red complex are actually found to be present in low numbers. More recently, multiple analyses of the human microbiome have started to shift the focus on biofilms away from consideration as a true “infection” but instead as a dysbiotic disease. We are beginning to live in the age of the dysbiotic inflammatory disease. Dysbiosis is a process by which communities of normally healthy bacterial species become unstable and unregulated and in response drive the inflammatory process. This outlook has become more optimal a term to assign to periodontal disease than just giving few species the honor of being disease causing agents. In healthy individuals, oral microbiota remains in a state of harmony and regulation, but in susceptible individuals or compromised patients, dysbiosis can lead to unfavorable and harmful host-microbial interactions and eventually leads to periodontal inflammation and destruction of the periodontal

tooth supporting structures [41-43]. This in turn leads to the inflammatory reaction products being released into the gingival crevicular fluid (CGF) which then promulgates and promotes furthering the disease process [44-46]. This cycle of inflammation and dysbiosis could be a key factor that plays into periodontal disease's main components, its lasting effects and difficulty to treat. Traditional therapy of scaling and root planning for periodontal disease, along with debridement and maintenance of the oral cavity may now be possibly augmented to include adjuvant therapies that target this dysbiotic shift towards more pathobiont species [47, 48]. In addition to this potential benefit, some of released host factors or molecules could have utility as disease markers in patient treatment. This could serve to reflect a more accurate disease state or give a better indication of the level of periodontal inflammation and disease progression than was previously available by solely clinical examination [49].

The keystone pathogen hypothesis was posited as a result of new information coming to light in the field. Studies showed that conversely, relatively low level of the red complex species were actually present in biofilms, and in the mice bone loss model suspected periodontopathogens were only needed in small numbers to influence periodontal inflammation and bone loss [50, 51]. The small bacteria cell count were enough to initiate a shift in the number and makeup of the complex biofilm. This alteration of the biofilm composition occurred before the onset of significant bone loss and was closely associated with the colonization of *P. gingivalis*, indicating that the cause of the disease was the shift in bacterial species

composition or dysbiosis not solely the offending organisms' presence alone [51]. This in conjunction with the observed fact that *P. gingivalis*, in the absence of other commensal bacteria, fails to cause periodontitis in mice. For the purposes of this dissertation, our discussion will focus mainly on the periodontopathogen and keystone pathogen, *P. gingivalis*, its associated virulence factors, and the methods by which these are manufactured and undergo post-translational modifications.

Porphyromonas gingivalis

P. gingivalis, as mentioned above, has been a heavily studied pathogen in the oral cavity and will be mainly the subject of this dissertation. As mentioned previously we label this bacterium as a keystone pathogen in human periodontitis [50, 52]. By placing this moniker on this bacterium, we imply that this organism is capable of causing dysbiosis. The dysbiosis can manifest in the form of either relative number or abundance of pathogenic species or change in the role or stratum of the species within the biofilm, even at low microbial levels within the biofilm. Microbial analysis studies have shown that despite its known importance in oral biofilm, *P. gingivalis* is only a minor constituent of periodontal disease-associated biofilms [53-55]. This is further confirmed by studies showing that, in a mouse model of periodontitis, *P. gingivalis* was able to colonize in low-levels and was shown to cause an increase in certain populations of the periodontal microbiota followed by inflammation-driven alveolar bone loss [51]. In addition, serving as a keystone pathogen comes with certain responsibilities such as serving a specialized role in the biofilm community. This role coordinates and modulates the activity of other organisms within the plaque and plays an essential role in its pathogenicity [56, 57]. In this

role, *P. gingivalis* influences the transition from mainly commensal bacteria into a pathogenic biofilm [52]. *P. gingivalis* is a Gram-negative, obligate anaerobe, and asaccharolytic rod which possess a number of virulence factors [58-60]. Many of these virulence factors are directly related to *P. gingivalis*' ability to subvert the host immune system. The use of these virulence factors is what makes *P. gingivalis* an effective pathogen.

Gingipains

Some of these virulence factors alluded to previously are the proteases, gingipains. Included in this category are the arginine-specific gingipains [Arg-gingipain-A (RgpA) and Arg-gingipain-B (RgpB)] and also the lysine-specific gingipain [Lys-gingipain (Kgp)]. These are encoded respectively by their three constituent genes within the *P. gingivalis* chromosome commonly referred here as *rgpA*, *rgpB* and *kgp* which are heavily conserved among different clinical and experimental strains of *P. gingivalis* [61]. The products of the translation of these genes (specifically the *rgpA* and *rgpB*), RgpA and RgpB, both contain a caspase-like domain (that retains specificity for Arg-Xaa peptide bonds) and an immunoglobulin-like domain. Uniquely in the proteinase RgpA, the protease and Ig-like domain is subsequently followed-up with a large hemagglutinin-adhesin C-terminal extension. Closely related to the above protein, the *kgp* gene-translation product, Kgp, contains a catalytic domain specific for Lys-Xaa peptide bonds and also contains a hemagglutinin-adhesion domain not too unlike the *rgpA* translation product. [62, 63], RgpB lacks the hemagglutinin-adhesin domains but the short C-terminal domain is conserved. Gingipain translation products undergo heavy post-

translational modification. Nascent translation products encompass a pro-fragment, a catalytic domain, an Ig-like domain, hemagglutinin-adhesion domains (only in RgpA and Kgp) and the conserved C-terminal domain (CTD). During secretion of RgpB, the pro-fragment is proteolytically removed and subsequent processing of the CTD reveals the active catalytic domain followed by the Ig-like domain. Subsequent glycosylation and incorporation to the outer membrane surface occurs afterwards. In the case of RgpA and Kgp similar processing occurs but the hemagglutinin-adhesin domains remain non-covalently associated with the catalytic domain. Lastly, gingipains once processed are secreted either as a monomeric form specific to the case of RgpB, or as complexes of protease and hemagglutinin-adhesin domains in the case of RgpA and Kgp. These complexes are either predominantly attached to the bacterial surface or released into the medium in a soluble form. This is dependent on a *P. gingivalis* strain, for example the strain HG66 secretes soluble gingipains freely into the media. Gingipain activities serve as mediators for nutrient acquisition, serve to cleave receptors on the host cell surface, and moreover, avoid and subvert the host immune system by inactivation of cytokines and components of the complement system. One of the most profound changes observed in patients with clinical periodontal disease is the aberrant remodeling of the host periodontal tissues. Structural changes that are often associated and observed with advanced periodontal disease include alveolar bone resorption and periodontal ligament destruction. These changes in structure in turn lead to attachment loss and periodontal pocket formation and eventually tooth loss. Periodontal pockets found in patients with periodontal

disease are also lined with epithelial cells that have had alterations, making them distinctly different from healthy cells that form the junctional epithelium found in the healthy periodontium. To accomplish this tissue-remodeling host cells require proteolytic degradation of important structural elements and extracellular matrices such as the collagen fibers forming the periodontal ligament and proteins involved in cellular junctions and extracellular matrix proteins [64-67]. The mechanism by which gingipains play a role in this process is complex and beyond the scope of this introduction. But in summary gingipains are important both directly and indirectly involved in the pathological tissue remodeling associated progressing disease process of periodontitis. Nevertheless, it is most likely that gingipains are not solely involved as the major virulence factor in periodontal disease tissue destruction [59]. It is instead much more probably that these proteases synergize with other mechanisms and virulence factors used by *P. gingivalis* and other bacteria and disrupt the host proteolytic balance and interfere with endogenous host protease inhibitors. Once this balance has been disrupted, host proteases, namely MMPs, TIMPs, and neutrophil elastase, drive the response in the periodontium for accelerated remodeling and pathological destruction of the host tissues[64, 68]. The effects of gingipains have been studied in great details and the role that they play in the disease process is expanding [59]. This variable output of potent virulence factors gives *P. gingivalis* quite an arsenal with which to exert effects into the host organism and biofilm community.

Protein Secretion Systems of *Bacteroidetes* Species

Apart from the Sec pathway that exports proteins into or through the inner membrane [69, 70], the armamentarium of well-characterized secretion pathways of *Bacteroidetes* is surprisingly limited. *Bacteroidetes* possess both type 1 and type 6 secretion systems (T1SS and T6SS) that are responsible for secreting proteins to extracellular environment bypassing the periplasm. Recently, there has been a great deal of effort produced to characterize the T9SS. This system is typical for *Bacteroidetes* and rarely, if ever, found outside the phylum [71, 72]. The T9SS machinery transports proteins across the outer membrane, which were first exported into the periplasm via the Sec translocon. All proteins secreted by T9SS possess a characteristic C-terminal domain (CTD) that codes for transportation through the outer membrane [71, 73]. The processes that are undertaken upstream of CTD-dependent secretion have garnered less investigation, mainly due to their ubiquity in other organisms and *Bacteroidetes* and have been extensively studied in gram-negative bacteria in general [70]. We report here that these upstream processes are unique to *Bacteroidetes* and do in fact merit attention. To put this more into perspective, some background on the Sec translocon is helpful.

The Sec pathway identifies target proteins by the presence of a signal peptide [74]. These signal peptides contain a tripartite architecture. They consist of a positively charged N-terminal region, which is thought to designate proteins to the phospholipid membrane, a hydrophobic region, which is hypothesized to be inserted into the membrane, and finally a shorter region that often contains a

consensus motif for a signal peptidase [75, 76]. Proteins that contain signal peptides can escape from the Sec translocase in two different ways. If they manage to escape “laterally”, they will then become contained within the inner membrane [69]. The other way would have them reach the periplasm, but the signal peptide portion is not cleaved and remains in the inner membrane. This leaves the proteins’ C-terminal end (with a signal peptide cleavage site) exposed on the periplasmic surface of the inner membrane [75]. The eventual fate of proteins that reach this stage will depend on the type of the signal peptide contained within.

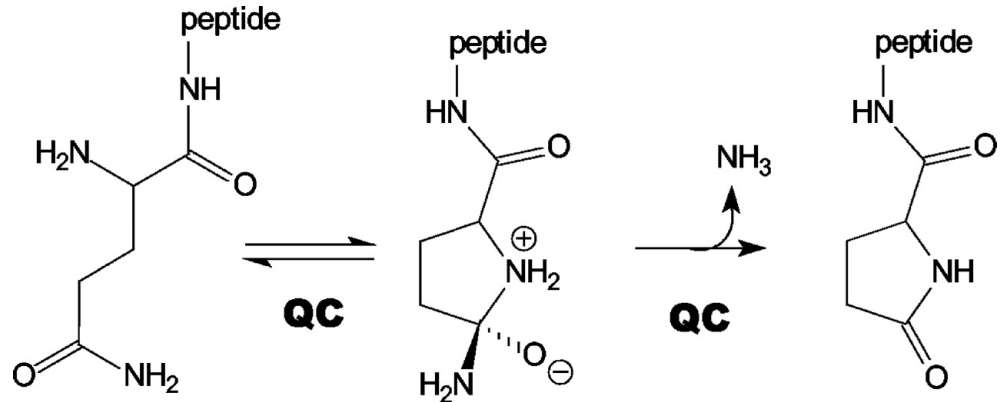
Proteins that carry a type I signal peptide are released from their membrane anchored signal peptide by signal peptidase I (SPI) [74, 75]. They will subsequently remain in the periplasm, or if necessary be transported further, for example, by a T9SS through the outer membrane, ultimately destined for the surface of the outer membrane or for release into the environment [71]. Proteins which carry a type II signal peptide undergo processing differently. A diacylglycerol transferase (termed Lgt) first attaches a diacylglycerol membrane anchor to the cysteine residue which resides immediately downstream of the signal peptide [77]. Secondly, signal peptidase II (SPII) (also known as lipoprotein signal peptidase or Lsp) can cleave a lipoprotein upstream of the modified cysteine residue [78, 79]. Occasionally, lipoproteins can remain attached to the inner membrane while others are transported to the outer membrane via the Lol system [80]. Thus, lipoproteins

found in gram-negative bacteria are generally periplasmic proteins which are anchored either to the inner or outer membrane of the bacteria.

The N-terminal residue of proteins is frequently chemically modified, and these modifications often have a signaling role. If an N-terminal glutamine residue is exposed as a result of proteolysis, these glutamine residues have the capability to spontaneously cyclize to pyroglutamate, with concomitant release of ammonia as a side product. The reaction is also facilitated by inorganic catalysts such as phosphate ions serving as the proton shuttle, and furthermore, can be catalyzed enzymatically by glutaminyl cyclases (QCs) [81].

Glutaminyl Cyclase

As one of the enzymes for protein post-translational modifications, glutaminyl cyclase (QC; glutaminyl-peptide cyclotransferase (QPCT), EC 2.3.2.5) is an acyltransferase that catalyzes N-terminal pyroglutamate (pGlu) formation on proteins or peptides and the concomitant release of ammonia or water molecules see Figure 1 [82].



Stephan Schilling et al. J. Biol. Chem.
2003;278:49773-49779

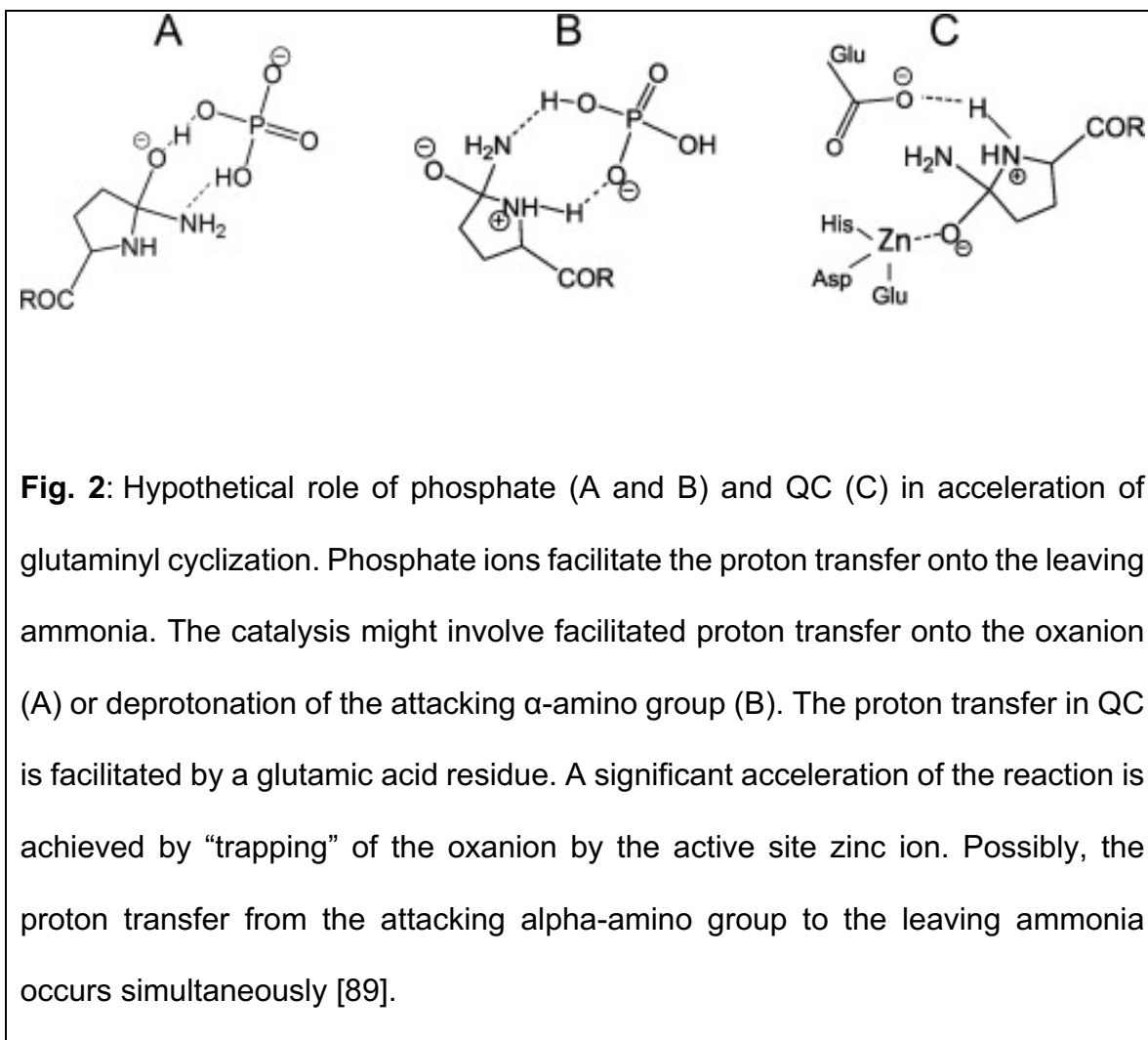
©2003 by American Society for Biochemistry and Molecular Biology

JBC

Fig. 1: N-terminal cyclization of glutamyl peptides by QC. Glutamyl containing peptide is cyclized in the presence of QC by formation of an intermediate state that culminates in the release of ammonia.

The cyclization of L-glutamine into pyroglutamate is considered a quasi-irreversible intramolecular acyl transfer reaction. The N-terminal peptide amino group is responsible for a nucleophilic attack on the γ -carbon amide, forming a tetrahedral intermediate. Subsequent decomposition of this intermediate occurs from net 1,3-proton transfer from $N\alpha$ onto a leaving ammonia, forming the pGlu ring. This cyclization or modification appears to be involved in the structural stability of secreted proteins, resistance to aminopeptidase degradation, and hypothetically play an important role in mediating receptor binding [83]. QC is a catalytically non-discriminatory enzyme; acting upon an available N-terminal glutamine residue, although it does exhibit slight preference for substrates containing a penultimate bulky hydrophobic residue [84]. Recently it has been shown that phosphate ions in conjunction with QC are able to operate as a coordinated proton transfer system. This system is able to effectively increase the rate of cyclization by QCs. Possibly; phosphate acts as a dual functioning acid–base catalyst to increase the proton transfer rate, where simultaneous protonation and deprotonation occur together in conjunction with a cyclic-ring transition state (Fig. 2 A and B). Previously phosphate ions have been hypothesized to serve as dual functioning catalysts during the iminolactone hydrolysis [85] or for thiamin enzyme tautomerization [86]. Acid–base catalysis is the primary source of catalysis used by QCs. The proposed role of the active-site zinc ion in QC can be nicely correlated to the above-described rate-limiting trapping of $T\pm$ in acyl transfer reactions in solution (Fig. 2 B). The active site zinc functions as a strong Lewis acid, and proton transfer from the attacking α -amino group to the leaving

ammonia is accelerated by a glutamic acid moiety in conjunction with two other acidic residues, as suggested by QC crystal structures [87, 88].



QC was originally discovered in dried latex belonging to the *Carica papaya* (CpQC) plant species [90]. Glutaminyl cyclases (QCs) have been demonstrated in multiple plant and bacterial species and share a common ancestry [91-94]. It has been

found that the known mammalian QCs are either Golgi-resident or freely secreted enzymes [93]. Several peptide hormones and proteins carry N-terminal pyroglutamyl residues. Until somewhat recently, the cyclization of L-glutamine peptides' N-terminus into pyroglutamate was thought to occur spontaneously [95]. This cyclization was shown that the conversion occurs under physiological conditions but at a very slow rate, therefore necessitating the need for enzyme catalysis [96]. Mammalian and plant QCs, however, have been discovered to serve as this executor of the reaction [97-101]. In general, both mammalian and plant QCs appear to have similar molecular masses, ~33 and ~40 kDa, respectively, and both are monomeric proteins [102, 103]. The primary structures of the proteins, however, display no sequence similarity, and the secondary structure of the individual QCs are completely different. The plant CpQC and the related QC from bacterial plant pathogen *Xanthomonas campestris* (XcQC) adopt a five-bladed beta-propeller fold [104]. As one would expect for beta-propeller proteins, the active site is located near the propeller axis [105]. Mammalian QCs however are shown to encompass an α/β -fold [106-108]. In addition, currently identified plant QCs do not share sequence homology to other known plant enzymes, which places them into a separate enzyme family or subfamily [100]. On the other hand, identified mammalian QCs possess clear homology toward known bacterial aminopeptidases, thus suggesting possible the evolutionary origin of the protein family [107]. The mechanism of catalysis for plant QCs is much less clear than for mammalian QCs. In mammalian QCs, the cyclization reaction serves its function during maturation of numerous cytokines and neuropeptides in the secretory

pathway, such as gonadotropin-releasing hormone (GnRH), thyrotropin-releasing hormone (TRH), and monocyte chemotactic protein-2 (MCP-2). The theoretical role of the pGlu residue on these peptides is believed to serve two functions; (1) protecting the peptides from peptidase degradation and (2) providing the proper conformation of the peptide to facilitate receptor binding [109, 110]. Uncontrolled expression of QC in humans (HsQC) has been shown to be related to certain pathological conditions, for example Alzheimer disease [111]. Site-directed mutagenesis and X-ray crystallography studies of recombinant HsQC have given us large amounts of information about the catalytic mechanism of QCs [112, 113]. Furthermore, HsQC has been used as a target for inhibitors, which have been synthesized and developed as drugs to treat the relevant diseases that occur from their overabundance [94, 114]. QCs have also been shown to be present in a number of snake venom isolates [115] in keeping with finding that proteins and toxins in snake venoms are often resistant to Edman-degradation during sequence analysis. Cases that have been shown include bradykinin-potentiating peptides [116, 117], metalloproteinase inhibitors [118], and endogenous metalloproteinases [119]. Based on current literature, human QC is thought to share the scaffold of known bacterial aminopeptidases [120]. This is in contrast to the fact that all the putative QCs thus far identified in bacteria share homology with plant QC. When analyzed by atomic absorption spectroscopy, HsQC has been shown to contain one zinc ion per HsQC molecule [121]. Competitive inhibitors of HsQC have been identified, such as heterocyclic compounds (imidazole, tetrazole, and triazole rings). This is most likely due to nitrogen atoms serving as good coordinators of

the active-site zinc ion found in QC [122, 123]. Solely the fact that HsQC could be inhibited/inactivated by heterocyclic inhibitors suggests that the zinc ion located within the QC is essential for catalytic activity [94]. In stark contrast, the same heterocyclic chelators display no inhibition of plant QCs [103]. Considering this information together, both plant and mammalian QCs are thought to belong to two different enzyme families with different ancestral origins [100]. While mammalian QCs are implicated in the maturation of numerous neuropeptides and cytokines, such as thyrotropin-releasing hormone (TRH) and gonadotropin-releasing hormone (GnRH) [102, 124, 125], the physiological function of plant QCs remains poorly characterized. Recently, it has been suggested that plant QCs could be involved in defense mechanisms [126, 127], a hypothesis that is supported by the observation that the quantity of plant QC expressed increases greatly as a result of repeated injury [127]. The role of QCs in both bacteria and parasites has not been studied in depth. Advances in methodology for QC activity assays [128] and the discovery of new HsQC inhibitors [114, 129] have rendered better tools to explore QCs. A new QC has been isolated from *P. gingivalis* and its role has been examined for the first time. Structural homology models of known QCs were generated and compared. Furthermore, we successfully cloned and sequenced the QC cDNAs from *P. gingivalis* and compared the sequence with that of human and other animal QCs. In addition, we also examined the optimal pH range, stability, and the effects of metal chelators, metal ions, and finally examined specific QC inhibitors on the representative bacterial QC. These QCs share similar catalytic activity but structurally remain distinctly different. [113, 126]

In studying the proteome of *P. gingivalis* and its novel T9SS, protein sequences destined for secretion via the T9SS with the conserved C-terminal domains (CTDs) that facilitate secretion from through the outer membrane complex [73]. Approximately 30 CTD-bearing proteins exist in *P. gingivalis* genome and these proteins all contain this conserved C-terminal domain [73]. Recently it has been demonstrated that the CTD-containing proteins are secreted and attached to the cell surface via the type IX secretion system (T9SS) [73, 130-132]. These CTD-bearing proteins undergo extensive post-translational modifications before attachment to the surface. Belonging to this group of CTD-containing proteins are the gingipains (RgpB, HRgpA, Kgp), which are major virulence factors of this periodontopathogen [133]. Upon examination of the sequences of these T9SS cargo proteins it can be observed that a N-terminal Gln residue is present just after the N-terminal signal peptide. Mass spectrometry analysis of these secreted proteins revealed that after post-translational modification, a pGlu residue is present at the N-terminus of the mature protein. This led us to hypothesize the existence of a bacterial QC present in *P. gingivalis*, responsible for this cyclization of Gln to pGlu. The presence of proteins containing N-terminal pyroglutamate residues has been noted in previous proteomic studies on *Bacteroidetes* species [73, 134-137]. At the outset of this study, we became aware of a drastic overrepresentation of glutamine residues after SPI cleavage sites in *P. gingivalis*. Starting from these two observations, we aimed to (1) clarify the pathway of pyroglutamate formation, (2) determine the fraction of SPI substrates that could be cyclized, (3) estimate the fraction that is actually cyclized, (4) test a possible role

of pyroglutamate formation in sorting, initially for *P. gingivalis* only, and then for *Bacteroidetes* in general, (5) characterize the function and importance of PgQC within the T9SS. The function and purpose of the PgQC is hypothesized. In this dissertation, we attempt to verify the existence, explain the purpose and role of QC in *P. gingivalis*, and reveal its potential importance in the secretion pathway in *P. gingivalis* and other *Bacteroidetes*.

CHAPTER II: MATERIAL AND METHODS

Proteomes and taxonomy information were taken from UNIPROT [138]. Signal peptides and cleavage sites were predicted using the batch version of SIGNALP4.1 [139]. Lipoproteins were predicted using LipoP1.0 [140]. Sequence logos were generated using the program Weblogo [141]. Intersections between proteins with predicted signal peptide and predicted lipoproteins were using the UNIX comm tool. Since not all UNIPROT species have been fully identified, some species names such as "*Tannerella sp.*" were encountered.

Cloning, expression and purification of recombinant PgQC

The QC protein was expressed as a GST-tag fusion protein. Briefly, the entire coding region of *qc* identified by BLAST search (PG_2157) was amplified from a *P. gingivalis* W83 genome template with Platinum Taq DNA Polymerase High Fidelity (Invitrogen) using primers F1_QC: ATTAGAATTCATGAAAAGACTGATAACAACAGGAG and R2_QC: ATTACTCGAGTCAGTGTGAAGCGGCTTTCACCTGTTTCG. The 1001 bp PCR product was digested with EcoRI – XhoI and cloned downstream in-frame with the sequence encoding glutathione S-transferase (GST), into EcoRI – XhoI digested pGEX-6P-1 expression vector (GE Healthcare). Following confirmation by PCR, resulting expression pGEX/QC vector was transformed into *E. coli* BI21 (DE3) expression host. Transformed *E. coli* cells were grown in LB media at 37° C until

OD₆₀₀ 0.6, cooled down to 24 °C and expression of recombinant protein was induced with 0.1 mM isopropyl-1-thio-β-galactopyranoside (IPTG). After overnight cultivation, cells were harvested by centrifugation (6,000 x g, 20 min), resuspended in PBS supplemented with lysozyme, and lysed by sonication (3 cycles of 10 x 3 s pulses at 17 W). Cell lysate was clarified by centrifugation (30,000 x g, 30 min) and loaded onto a pre-equilibrated glutathione-Sepharose™ High Performance column. Recombinant GST-QC fusion protein was eluted using 50 mM Tris-HCl, pH 8.0, supplemented with 10 mM reduced glutathione. The purified GST-QC protein was subsequently incubated with PreScission™ Protease (GE Healthcare) and subjected again to chromatography on glutathione-Sepharose™ to remove the GST tag. The purity of the resulting protein was verified by SDS-PAGE electrophoresis (NuPAGE^R 4-12% Bis-Tris Gel, Invitrogen). Protein concentration was determined by BCA Assay (Sigma).

PgQC activity assay

The activity of PgQC was determined essentially as previously described (33). Briefly, 150 µl of the assay buffer (40 mM Tris-HCl, 400 mM KCl, pH 8.0), 10 µl of chromogenic substrate (200 mM H-Gln-AMC in DMSO), and 10 µl of a recombinant bacterial pyroglutamyl aminopeptidase (25 U/ml, Unizyme Laboratories, Hørsholm, Denmark) were mixed together in a microtitration plate and preincubated 10 min at 30°C. The reaction was initiated by addition of 30 µl appropriately diluted purified rPgQC or *P. gingivalis* whole culture or washed

bacterial cells or subcellular fractions and after 1 min incubation the increase in fluorescence ($\lambda_{\text{ex}} = 380 \text{ nm}$, $\lambda_{\text{em}} = 460 \text{ nm}$) was recorded for 10-20 min at 30°C. Unspecific cleavage of the H-Gln-AMC substrate was determined by omitting pyroglutamyl aminopeptidase, the auxiliary enzyme. If necessary, the unspecific cleavage was subtracted from PgQC activity. Metal-ion inhibition reactions were carried out in similar fashion with each respective inhibitor added to the reaction mixture prior to initiation of the assay.

***P. gingivalis* culture and cell fractionation procedures**

P. gingivalis culture fractionation was performed at 4°C as described previously [142] starting from stationary-phase (a 2-day-old) cultures adjusted to an OD₆₀₀ of 1.5. Briefly, cells were collected by centrifugation at 6,000 × g for 15 min, washed once with phosphate-buffered saline (PBS), and resuspended in 5 ml of 0.25 M sucrose and 30 mM Tris, pH 7.6. After mixing gently for 10 min cells were repelleted at 12,500 × g for 15 min. The outer membrane was disrupted by the rapid addition of ice-cold distilled H₂O and the spheroplasts were pelleted by centrifugation at 12,500 × g for 15 min. The supernatant was designated the periplasmic sample. The remaining spheroplast pellet was resuspended in 5 ml PBS and ultrasonicated in an ice-water bath. Cellular debris and membranes were pelleted by ultracentrifugation at 150,000 × g for 1 h, and the supernatant was designated the cytoplasmic sample. The remaining pellet was washed and resuspended in cold PBS by sonication. This fraction was designated the

membrane sample. For individual membranes separation washed collected cells were lysed by ultrasonication as described above. The membranes were pelleted by ultracentrifugation (150,000 × g, 1 h) washed with PBS to remove periplasmic and cytoplasmic proteins and resuspended in PBS by sonication. The inner membrane was dissolved with Sarkosyl (lauryl sarcosine) and the residual Sarkosyl-resistant outer membranes (OM) were pelleted by ultracentrifugation (150,000 × g, 1 h). The supernatants were designated the IM samples while pellets washed and suspended by sonication in PBS were designated the OM samples. Purity of the various fractions was checked by Western blotting for A-LPS or gingipains and the biotin containing 15 kDa biotin carboxyl carrier protein (AccB alias MmdC or PG1609) as OM and IM specific markers, respectively [62, 143] (data not shown).

Generation of *P. gingivalis* Δ RgpB deletion mutant

For subsequent analysis, generation of plasmids suitable for *rgpB* gene mutagenesis the pRgpBall master plasmid was first engineered based on the pURgpB-E construct [142]. A partial *rgpB* gene section upstream of the erythromycin cassette was replaced with whole *rgpB* coding sequence, together with an 817 bp fragment containing its potential promoter. The new fragment was amplified with primers RgpBall_F and RgpBall_R using genomic DNA of *P. gingivalis* W83 and ligated into the linearized pURgpB-E plasmid (with EcoRI and

Small restriction enzymes) by the Gibson's method [144] resulting in pRgpBall-erm plasmid. All primer sequences are listed in Table 2.

pRgpBall-erm plasmid	
RgpBall_F	GACGGCCAGTGAATTCTTAACCAT GCTGTGGTGACGAG
RgpBall_R	AGCGGAAGCTATCCCAACAGTCT CTTGCGTAGTGCCAA
pRgpBdel-erm plasmid	
RgpBQ1N_Rs	AACGCCATTCCTCCCAACAG
RgpBdelFs	GGGATAGCTTCCGCTATTGCT
RgpBdelRt	GGGTCTGCCGGCTGTGCAAACGC CATTCTCCCAACAG
RgpBdelFt	TGCACAGCCGGCAGACCCGGGAT AGCTTCCGCTATTGCT
RgpBQ24N mutation	
RgpBQ1N_Fs	CGGTCGCAACCCACAAGTAC
RgpBQ1N_Ft	TGCAAACCCGGCAGAGCGCGGTC GCAACCCACAAGTAC
RgpBQ1N_Rs	AACGCCATTCCTCCCAACAG
RgpBQ1N_Rt	CGCTCTGCCGGGTTTGCAAACGCC ATTCTCCCAACAG
RgpBQ25A mutation	
Q25AF	GGAATGGCGTTTGCAGCTCCGGC AGAGCGCGGTC
Q25AR	GACCGCGCTCTGCCGGAGCTGCA AACGCCATTCC
pNRgpA-tet plasmid	
RgA_Up_F	GCCAGTGAATTCGGTCAGAGAGC CGA
RgA_Up_R	CGTTGTGGATCCTGAGCGTACCAT ATCTTTAACC
RgpA_Dw_F	TTGGCAGTCGACTCGAGGAGCTG ATTGGCTT
RgpA_Dw_R	TACCCAAGCTTGAGGAGCAGCA ATTG
Tet_BamHI_F	TCAGGATCCACAACGAATTATCTC CTTAAC
Tet_SalI_R	CGAGTCGACTGCCAAGTTCTAATG CTTC
puc_EcoRI_R	ACCGAATTCAGTGGCCGTCGT

puc_HindIII_F	CTCAAGCTTGGCGTAATCATGGT
RgpAQ25N mutation	
RgpAQ1N Fs	ACGCAATCCGAATGTGAGATT
RgpAQ1N Ft	GAACCAGACAGAGTTGGGACGCA ATCCGAATGTGAGATT
RgpAQ1N Rs	GCAAATGCCATTCTCCTAAT
RgpAQ1N Rt	CCCAACTCTGTCTGGTTCGCAAAT GCCATTCTCCTAAT
pNKgp-cep plasmid	
Kg_Up_F	AGCTTGCATGCACACACCCCGAT
Kg_Up_R	ATGGAAGCTTAAGTCAGTCCAGC ATGAGGAAG
Kg_Dw_F	ACTTGAGATCTTAACCTTGGTCTG CTCTAC
Kg_Dw_R	CCGGGGATCCTTCTACCGTAACGT C
CepA_F	GACTTAAGCTTCCATAGACGATGC CACACTG
CepA_R	GTTAAGATCTCAAGTCACCGATAG TGATAGTG
pUC_BamHI_F	TAGAAGGATCCCCGGGTACCGAG CT
pUC_SphI_R	TGTGTGCATGCAAGCTTGGCGTAA TCAT
KgpQ20N mutation	
KgpQ1NFs	CTTGATGCTCCGACTACTCGA
KgpQ1NFt	AATAGCGCCAAGATTAAGCTTGA TGCTCCGACTACTCGA
KgpQ1NRs	GCGTAAAGACCAACTCCCA
KgpQ1NRt	CTTAATCTTGGCGCTATTGGCGTA AAGACCAACTCCCA

Table 2: Primers used for construction of plasmids for *P. gingivalis* mutagenesis.

Next, the RgpB deletional plasmid (pRgpBdel-erm) was obtained by the truncation of pRgpBall-erm plasmid using the PCR based Site-directed, ligase-independent method (SLIM) [145] with primers listed in Table 2. With this approach, only the small fragment of 3' (154 bp) of *rgpB* CDS was preserved on the pRgpBdel-erm plasmid. The Δ RgpB strain was obtained in the homologous recombination event: the plasmid was electroporated into the *P. gingivalis* W83 strain and the positive

recombinant clones were selected with 5 µg/ml erythromycin. Proper recombination was verified by sequencing.

Generation of *P. gingivalis* gingipains Q mutants

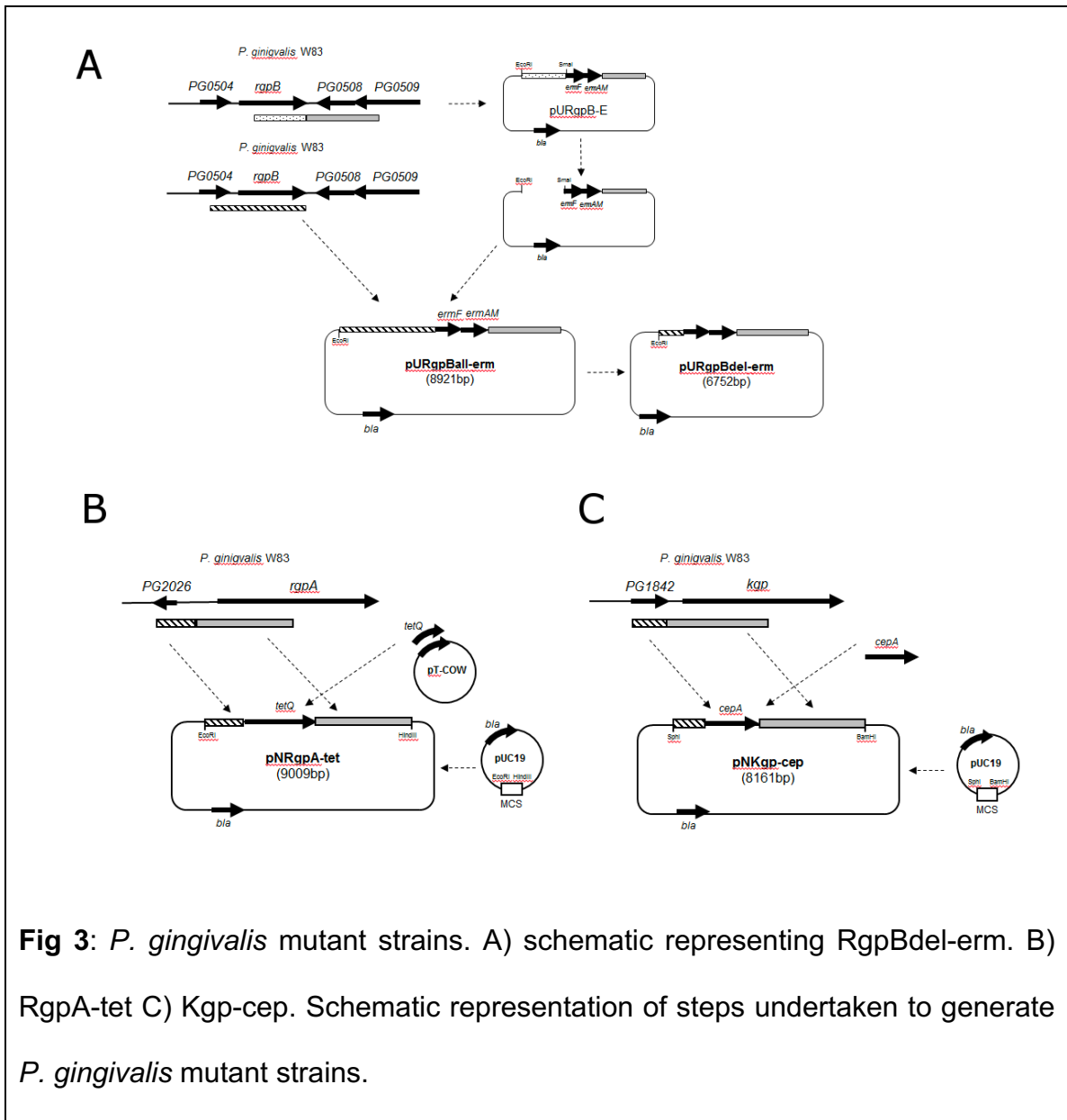
Mutagenesis of each gingipain required a dedicated master plasmid. For RgpB studies the pRgpBall-erm construct was used. The Q1N mutation (replacement CAG codon into AAC) was incorporated using the SLIM method (resulting in the pRgpBallQ1N-erm plasmid), the Q25A mutation (replacement of the CAG codon into GCT) was introduced by the QuikChange method (Stratagene) (generating pRgpBallQ25A-erm), all sequences of applied primers are listed in Table X in the RgpBQ1N section. These plasmids were introduced into the *P. gingivalis* W83 RgpA-C strain lacking the whole *rgpA* gene [142] by the electroporation and the recombined clones were selected with 5 µg/ml of erythromycin. The obtained strains were partially sequenced and named Δ RgpA/RgpBQ25N and Δ RgpA/RgpBQ25A, respectively.

For RgpA mutagenesis, a master plasmid pNRgpA-tet was engineered. Two DNA fragments were amplified from *P. gingivalis* genomic DNA. The upstream 915 bp fragment consisting of sequence directly adjacent to the RgpA promotor was amplified with primers RgpA_Up_F and RgpA_Up_R). A downstream 2835 bp fragment, comprising the 5' sequence of the RgpA gene together with 388 bp of its proposed promotor was amplified with primers RgpA_Dw_F and RgpA_Dw_R.

The tetracycline (tetQ) resistance cassette was amplified from the pT-COW plasmid [146] with primers Tet_BamHI_F and Tet_Sall_R. The backbone, the pUC19 plasmid, was linearized by PCR reaction with primers puc_EcoRI_R and puc_HindIII_F. All four amplified fragments were combined in the single step reaction by the method described by Gibson [144]. The Q24N mutation (replacement cag codon into aac) was incorporated to the construct with the SLIM method. Sequences of applied primers are listed in Suppl. Table 1 (RgpAQ24N section). This plasmid was introduced into the *P. gingivalis* W83 Δ RgpB strain lacking the whole rgpB gene by the electroporation and the recombined clones were selected with 1 μ g/ml of tetracycline. Obtained strain was partially sequenced and named RgpBdel/RgpAQ24N. The non-mutated master plasmid was also introduced into the Δ RgpB strain *P. gingivalis* W83 and the unaffected expression and activity of RgpA was observed.

For Kgp mutagenesis, the pNKgp-cep master plasmid was created in a similar manner. First, two fragments adjacent to the start of the hypothetical Kgp promotor were amplified from the genomic DNA, the 809 bp upstream fragment with Kg_Up_F and Kg_Up_R primers, while the 3271 bp downstream fragment with Kg_Dw_F and Kg_Dw_R primers. The beta-lactamase gene *cepA* was amplified with primers CepA_F and CepA_R from template synthesized by the Life Technologies based on the sequence deposited under AAA21538.1 number (Gene Bank). The pUC19 plasmid was linearized with primers pUC_SphI_R and pUC_BamHI_F. The Q20N mutation (replacement caa codon into aat) was

incorporated to the construct with the SLIM method. Sequences of used primers are listed in Suppl. Table 1 (KgpQ20N section). This plasmid was introduced into the wild type *P. gingivalis* W83 by the electroporation and the recombined clones were selected with 2 µg/ml of ampicillin. Obtained strain was partially sequenced and named KgpQ20N. As a control, the non-mutated master plasmid was also electroporated into the *P. gingivalis* W83 strain and the unaffected expression and activity of Kgp was observed.



Gingipain activity assay

The amidolytic activities of Rgp and Kgp enzymes were assessed by the hydrolysis of the chromogenic substrate benzoyl-L-arginine-p-nitroanilide (BAPNA) and carboxybenzoyl-L-lysine p-nitroanilide (zKpNA; Novabiochem, Germany), respectively. In a 96-well format, 20- μ l samples were preincubated in assay buffer

(200 mM Tris-HCl, 100 mM NaCl, 5 mM CaCl₂ [pH 7.6][71], supplemented with fresh L-cysteine to 10 mM) for 2 min prior to the addition of 1 mM substrate in a total volume of 200 μ l. For activity measurement of Sarkosyl-treated membrane fractionations (see Materials and Methods), a 0.125 mM concentration of a synthetic arginine substrate pyro-glutamyl-glycyl-L-arginine-p-nitroanilide (pyroEGRpNA; Pharmacia-Harper, Uppsala, Sweden) was used instead of BApNA due to precipitation of the BApNA substrate in the presence of the Sarkosyl detergent. The presence of 0.1% Sarkosyl detergent in the assay did not affect the rate of substrate hydrolysis as determined with purified RgpB (data not shown). The rate of formation of p-nitroanilide was measured at 405 nm using a SpectraMax Plus spectrophotometer (Molecular Devices Inc., CA). For ease of comparison between mutants and statistical analyses of independent repetitions, activity units were defined as the total activity present in the RgpB⁺ control mutant culture equaling 100 U for culture partitioning studies, the total activity in the RgpB⁺ control mutant cells equaling 100 U for cellular fractionation studies, or the total activity in the RgpB⁺ control mutant membranes equaling 100 U for membrane fractionation studies.

***In vivo* QC specific inhibition**

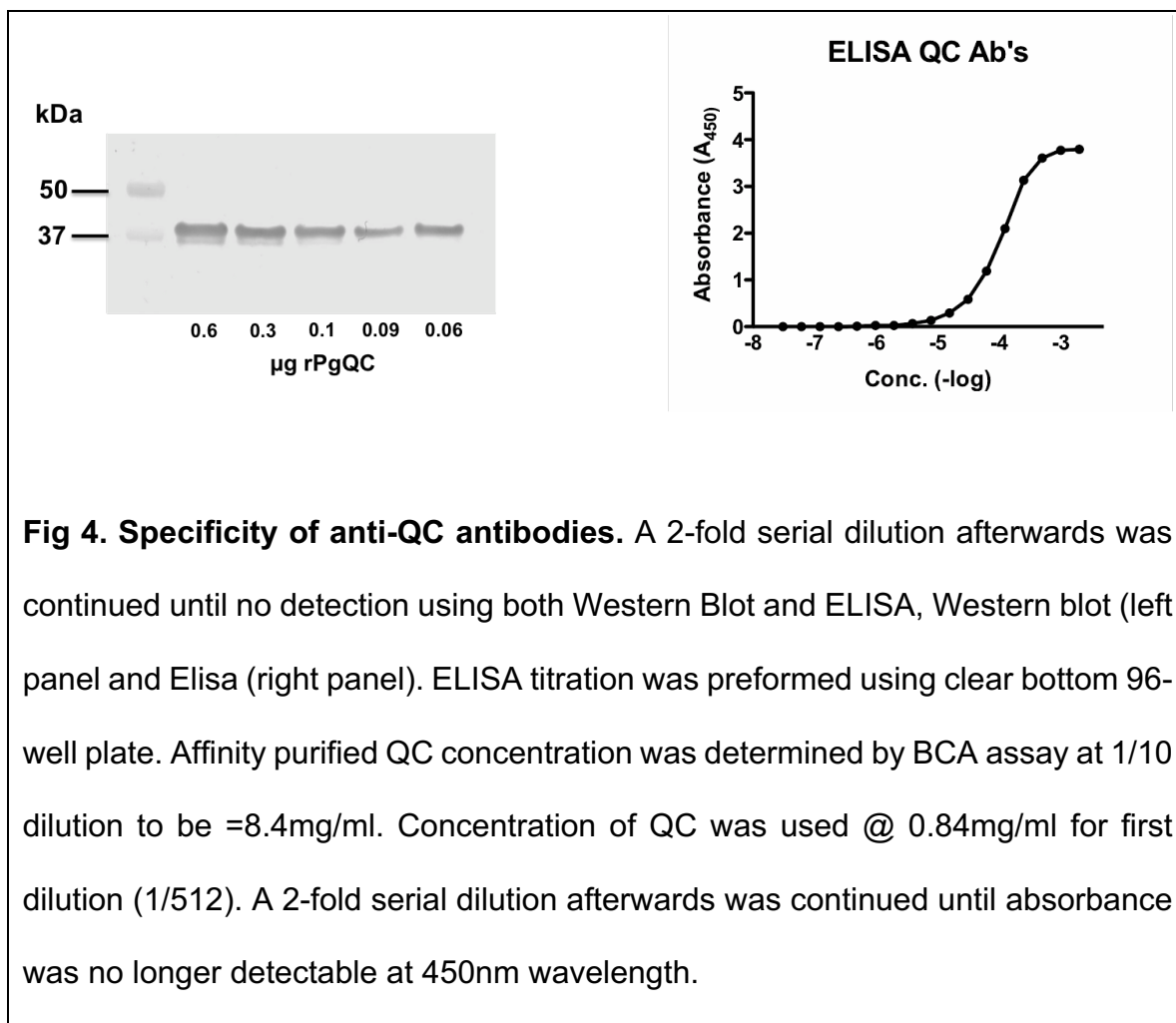
Each inhibitor was dissolved in DMSO at 10mM and 100mM concentrations. Five ml of a stock culture of *P. gingivalis* was equilibrated to OD₆₀₀ = 0.1 in 3 separate sealed tubes of 5ml of eTSB media (experiment repeated in triplicate). These tubes

are of the correct diameter to be read using the spectrophotometer cuvette reader. At inoculation either inhibitor concentration of 100 μ M or 1mM final concentration (DMSO content \leq 1%) was added or equivalent DMSO \leq 1% alone. Inoculated cultures of *P. gingivalis* were subsequently placed in an anaerobic chamber. Samples consisting of 1.0ml of bacteria were retrieved at 2, 5, and 8 hours post-inoculation. Samples were then centrifuged, supernatant was decanted, cell fraction was washed twice with PBS to remove unbound excess inhibitor. Bacterial pellet re-suspended in 300 μ l PBS and lysed by sonication (3 pulses, 5 s/pulse). Eighty μ l of lysate used for continuous spectrophotometric assay of glutaminy cyclase as previously described.

Affinity purified anti-QC Antibodies

CNBr-activated Sepharose 4B (GE Healthcare Lot # 10039621) was prepared according to manufacturer's specifications. CNBr-activated Sepharose 4B is a pre-activated resin using the cyanogen bromide method, which couples antibodies or other large proteins containing -NH₂ groups to the Sepharose media, without an intermediate spacer arm. rPgQC was dissolved in coupling buffer (0.1 M NaHCO₃ containing NaCl 0.5 M) at 5mg/ml of CNBr gel. CNBr beads were washed and swelled on a sintered glass filter. rPgQC protein solution mixed with swelled gel suspension in an end-over-end mixer for 2 hours at room temperature or overnight at 4°C. Remaining active groups were blocked by addition of blocking agent 1.0 M ethanolamine or 0.2 M glycine at approximately pH 8.0 (2 hours at room

temperature or overnight at 4°C). Excess protein was washed away by at least 3 alternating washes of coupling buffer and acetate buffer (0.1 M pH 4.5 containing 0.5 M NaCl). Blocking agent was removed with 3-4 washes of coupling buffer followed by storage buffer (PBS containing preservative NaN₃). Serum passed through 0.45µm filter prior to application to the column. Serum was loaded into the column, column washed with PBS until A₂₈₀ reached baseline. The antibody bound to the column is eluted with 0.1M Glycine-HCl, pH 2.8. Fractions collected into tubes containing 1.0M Tris pH 8.0, to neutralize the eluted antibody. Antibody fractions were pooled and dialyze vs. PBS and finally concentrated. ELISA was run on serum, flow-thru, and eluate (Fig. 4).



SDS-PAGE and Western Blots

Samples were analyzed using established protocols ([133]). Samples were first boiled in non-reducing SDS-PAGE sample buffer containing 2mM TLCK for 5 min to inactivate all gingipains prior to the addition of 1% β -mercaptoethanol and boiled for a further 5 min for complete denaturation. Samples were centrifuged briefly at 13,000 \times g, 1 min to remove particulates and the supernatant separated on SDS-PAGE and gels were stained with Coomassie Brilliant Blue. For Western blot analysis resolved proteins were subsequently electrotransferred onto 0.22- μ m-

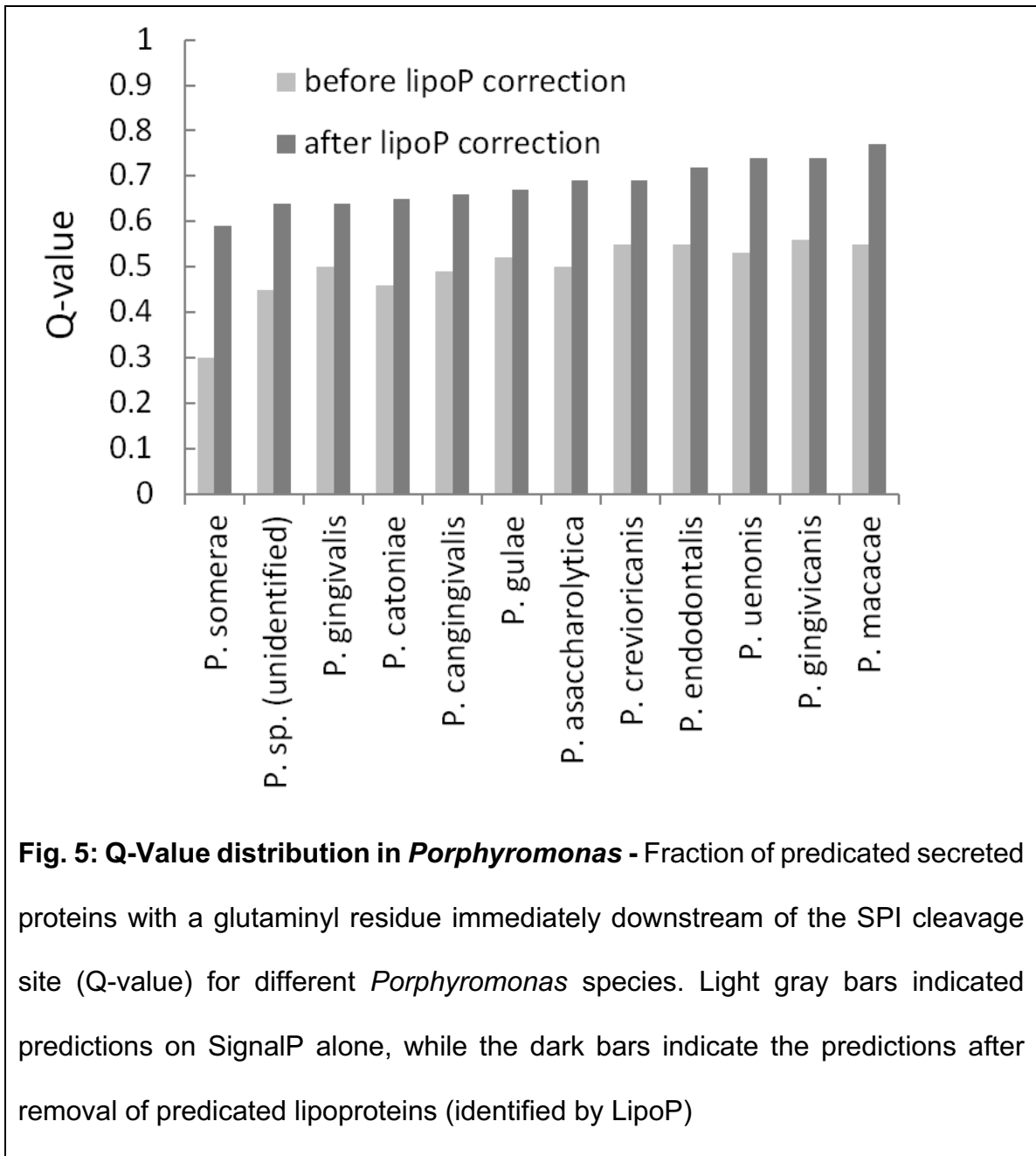
pore-size nitrocellulose membranes and blocked in 2% BSA/PBS solution overnight. RgpB was detected using a 1:2000 dilution of anti-RgpB mouse mAb in TTBS (20mM Tris, 500mM NaCl, pH 7.5 supplemented with 0.1% Tween 20) for 3 h. Membranes were washed four times with TTBS before being probed for 2 h with a 1:2000 dilution of an alkaline phosphatase-conjugated rabbit anti-mouse polyclonal secondary antibody (Dako Cytomation, Denmark). Development was carried out using the AP Conjugate Substrate kit as per manufacturer's instructions (Bio-Rad Lab., CA, USA). The *in vivo* PgQC and recombinant PgQC was detected using a 1:100,000 dilution ($1\mu\text{g ml}^{-1}$) of affinity purified specific (previously described) anti-QC rabbit polyclonal antibody in 5% (w/v) skim milk/TTBS solution. Membranes were washed four times with TTBS before being probed for 1 h with a 1:40,000 dilution of an HRP-conjugated rabbit anti-mouse polyclonal secondary antibody (Sigma-Aldrich). Development was carried out using the chemiluminescent protocol according to manufacturer's specification

CHAPTER III: RESULTS AND DISCUSSION

***Bacteroidetes* SPI substrates typically have a QIn (Q) downstream of the SPI cleavage site**

The starting point for this study was the observation that many secreted *P. gingivalis* proteins with a predicted signal peptide also had a glutamine (Q) residue immediately downstream. The generality of this observation was confirmed on a genome-wide basis using the batch version of SignalP (for gram-negative bacteria). These species designations were pooled into “superspecies” groups, with particularly well-defined Q-values, and an anomalously large number of predicted proteins with predicted signal peptides or type I signal peptides. In none of the analyzed species groups, the “superspecies” exceeded 15% with exception of *Cyanobacteria*, where 31% species were incompletely designated, often without clear signs that several species were pooled (judging from the number of proteins). Including the “superspecies”, 337 *Bacteroidetes* species, 13 *Chlorobi* species, 59 *Spirochaetes* species, 13 *Chlamydia* species, and 82 *Cyanobacteria* species were analyzed. The number of proteins with predicted signal peptides was above 50 in all analyzed species, guaranteeing that incomplete proteomes did not have a major influence on Q-values. The medium number of proteins with predicted signal peptides was 399 for the *Bacteroidetes*, 125 for *Chlorobi*, 163 for *Spirochaetes*,

128 for *Chlamydiae*, and 195 for Cyanobacteria. Removal of lipoproteins from the set of proteins with predicted signal peptides was a relatively “small correction”. The median values of the number of proteins with predicted type I signal peptides per species were 299 for the *Bacteroidetes*, 104 for *Chlorobi*, 146 for *Spirochaetes*, 112 for *Chlamydiae*, and 161 for *Cyanobacteria*. As lipoproteins have a C after the SP_{II} cleavage site, their removal always increased predicted species Q-values. A “Q” immediately downstream of the signal peptide was predicted in about half of the cases. In the remaining cases, the residue after the signal peptide was frequently a cysteine, suggesting that these proteins were lipoproteins/SP_{II} substrates. We used LipoP to identify and remove these proteins from the set. In the remaining set, which should only contain SPI substrates, the fraction of proteins with a Q after the SPI cleavage site exceeded 60%. Additional manual checks, including checks with earlier versions of the SignalP program, suggested that the true fraction of SPI substrates with a Q directly after the cleavage site may be even higher (Fig 5).



The enrichment of glutamine downstream of the SPI cleavage site did not appear to be specific for the proteins of a particular cellular compartment. CELLO [147] predictions identified SPI substrate proteins in the inner membrane, the periplasm, the outer membrane, and the extracellular space. In all compartments, the fraction of SPI substrate proteins with a Q immediately downstream of the SPI site was

48% or higher (Table 3), clearly indicating that Q enrichment was not characteristic for proteins of a specific compartment. Placement of some SPI client proteins in the cytoplasm by the CELLO server suggests that some predictions are in error. Even with this reservation, Q enrichment does not appear to be characteristic for SPI client proteins in a particular compartment. This conclusion was further strengthened by the inspection of protein lists.

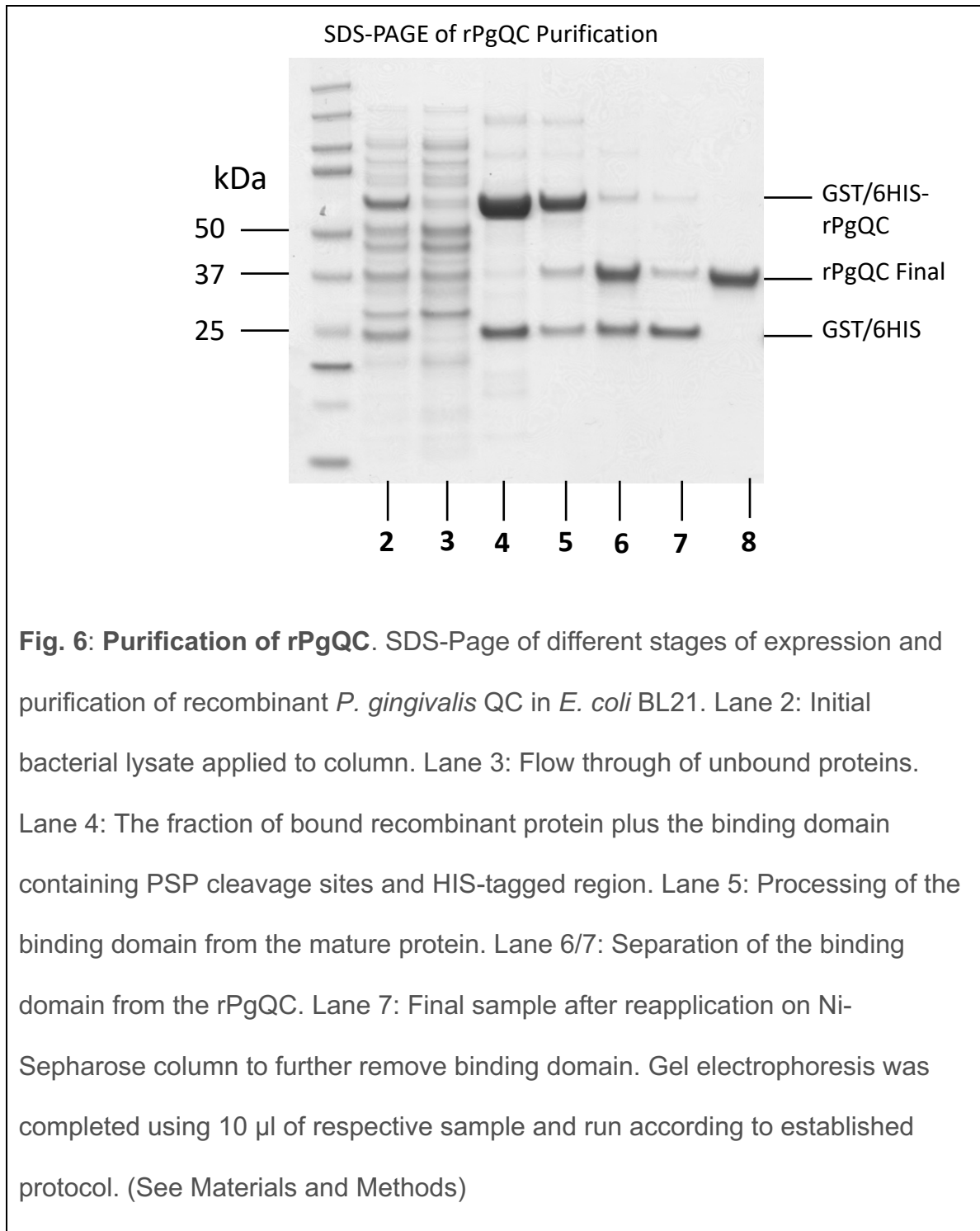
	<i>P. gingivalis</i>			<i>T. forsythia</i>		
	Q	Non-Q	Total	Q	Non-Q	Total
Extracellular	10 (56%)	8	18	13 (39%)	20	33
OuterMembrane	29 (48%)	31	60	54 (58%)	39	93
Periplasm	18 (58%)	13	31	34 (43%)	46	80
InnerMembrane	8 (100%)	0	8	6 (60%)	4	10
Cytoplasm	25 (50%)	25	50	41 (49%)	43	84
All compartments	90 (54%)	77	167	148 (49%)	152	300

Table 3: CELLO Predictions - Proteins with or without Q residue in P1' downstream of a type I signal peptide according to their localization, predicted by CELLO program.

Recombinant *P. gingivalis* PG2157 has QC activity and resides in the inner membrane

The high frequency of newly exposed Q residues in SPI substrates in *P. gingivalis* and the previously reported detection of 7 *P. gingivalis* proteins with N-terminal pyroglutamate [134] suggested that glutamine cyclization might not be

spontaneous, but enzymatically catalyzed. A BLASTP query of the *P. gingivalis* proteome with the human QC sequence suggested that PG2157 (also called PG_RS09565) may have QC activity. The recombinant protein (without a signal peptide) did not exhibit aminopeptidase activity on any of the commercially available substrates of general formula $\text{NH}_2\text{-L-Xaa-pNA}$ or $\text{NH}_2\text{-L-Xaa-AMC}$. However, it efficiently converted the fluorogenic substrate L-glutamyl-AMC into its respective pyroglutamic acid derivative ($K_m = 0.473 \text{ mM}$, $k_{\text{cat}} = 0.356 \text{ s}^{-1}$, $k_{\text{cat}}/K_m = 1.34 \text{ mM}^{-1}\text{s}^{-1}$). We therefore refer to PG2157 (PG_RS09565) as PgQC and to the recombinant version of the protein as rPgQC. SDS-PAGE of purification of rPgQC shown in Fig. 6.



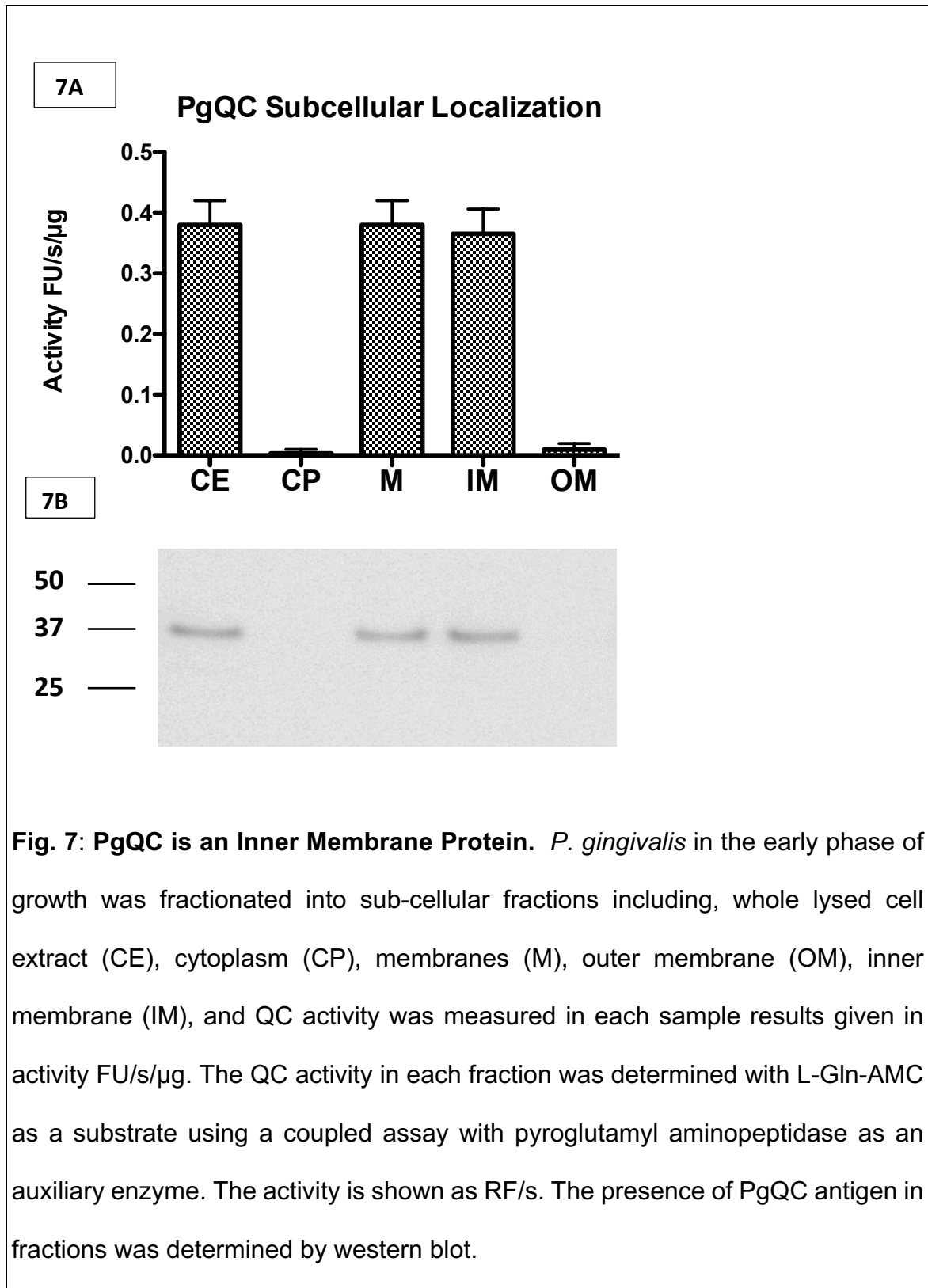
Species	H-Gln-AMC		
	K_m (mM)	K_{cat} (s ⁻¹)	K_{cat} / K_m (mM ⁻¹ .s ⁻¹)
<i>Porphyromonas Gingivalis</i>	0.473 ± 0.004 ^α	0.356 ± 0.02 ^α	1.34 ± 2 ^α
Human QC	51.3 ± 3	5.4 ± 0.1	98.0 ± 2 ^β
Human IsoQC	0.017 ± 0.001 ^γ	1.07 ± 0.03 ^γ	63 ± 6 ^γ
Murine QC	0.048 ± 0.003 ^δ	6.0 ± 0.2 ^δ	125 ± 4 ^δ
Murine IsoQC	0.030 ± 0.006 ^ε	6.98 ± 0.35 ^ε	322 ± 27 ^ε

Table 4: rPgQC Enzyme Kinetics

Michaelis/Menton kinetic parameters showing that, indeed, rPgQC is a glutaminy cyclase with much lower affinity for H-Gln-Xaa-Xaa than human or murine QC
^α(Determined in our lab) ^β([108]) ^γ([94]) ^δ([92]) ^ε([83])

Sequence analysis of PgQC revealed a canonical signal peptide with the typical lipobox (Leu-Ser-Ala-Cys), suggesting that PgQC is a lipoprotein. Lipoproteins are translocated across the inner membrane via the Sec system, and initially anchored to the inner membrane by covalent attachment of a lipid anchor to the cysteine residue, followed by signal peptide cleavage, and typically second N-acetylation. Some, but not all lipoproteins are subsequently transferred from the inner to the outer membrane. Therefore, we expected that PgQC should be anchored in the inner or outer membrane.

In order to determine QC localization experimentally, cell extract (CE) of *P. gingivalis* in late exponential/early stationary phase of growth was fractionated into cytoplasm and periplasm (CP), total membranes (M), outer membrane (OM), and inner membrane (IM). The purity of the membrane fractions was verified by the exclusive presence of the biotin-containing 15-kDa biotin carboxyl carrier protein (AccA alias MmdC or PG1609) and gingipains in the IM and OM, respectively [136] (data not shown). QC activity of the fractions was then measured using the enzyme-coupled assay already used previously to demonstrate the activity of the recombinant enzyme. QC activity was found in the IM and in fractions containing IM (CE and M) but not CP and OM (Fig. 7A) clearly indicating that PgQC is anchored in the inner membrane. This localization was further confirmed by Western blot analysis of enriched subcellular fractions using rabbit polyclonal antibodies anti PgQC (Fig. 7B).



***Porphyromonas gingivalis* QC is a zinc metalloenzyme**

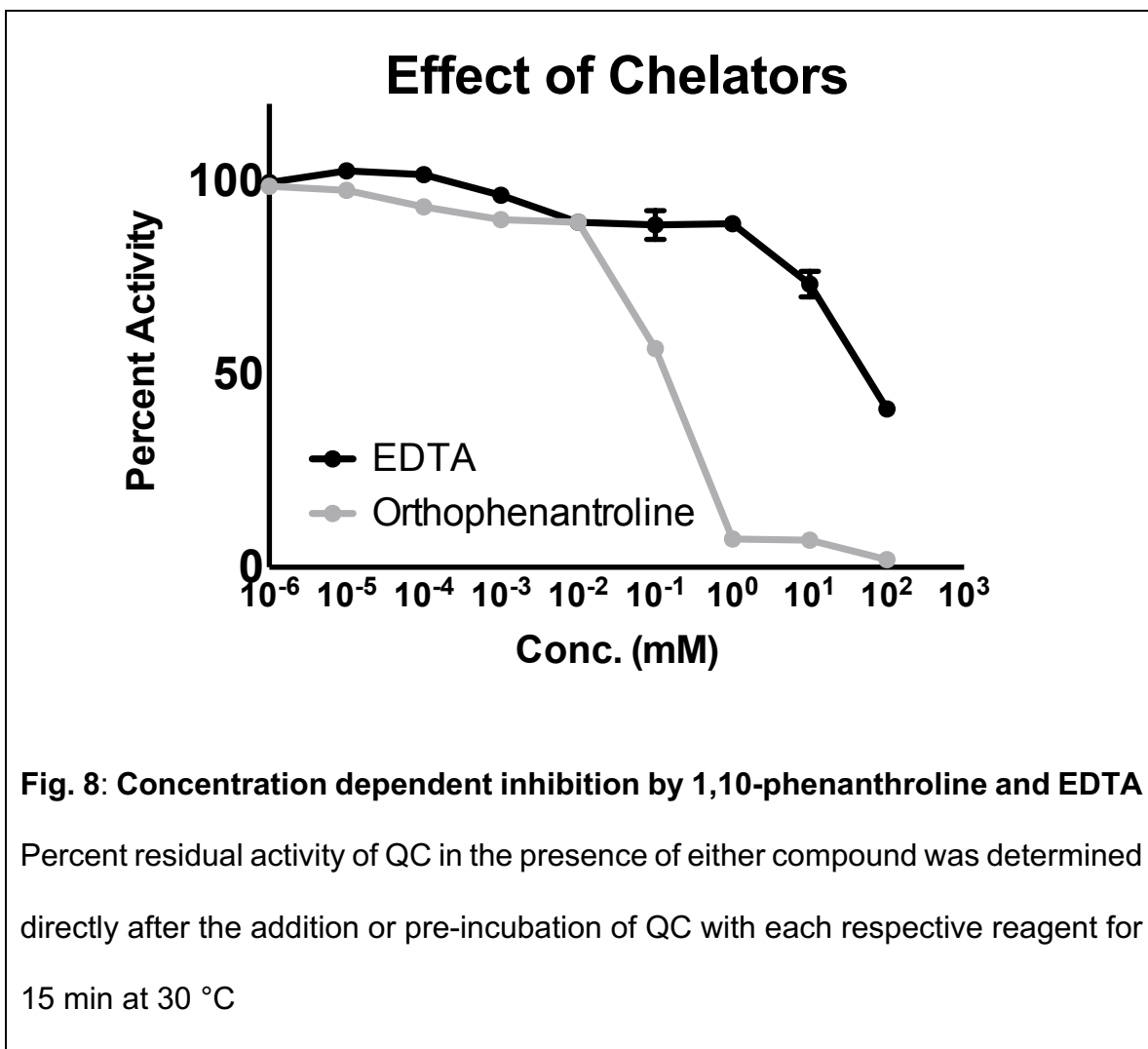
Previously, the metal ion content of human QC was unclear. Schilling et al. proposed that human QC is a metalloenzyme based on the inhibition by several metal ion chelators and the reactivation of apoenzyme by the subsequent addition of zinc ions [92]. However, Booth and co-workers reported lower than 0.3 molecule zinc ion per hQC molecule which was shown by mass spectrometry [120]. Because neither the accessory enzyme for the reaction, pyroglutamyl aminopeptidase, nor glutamic acid dehydrogenase, is inhibited by imidazole within the concentration range used, both the fluorimetric and spectrophotometric assay were well adapted for our purposes. The fluorimetric activity assay data (Table 5) revealed inhibition by imidazole. Imidazole completely blocks substrate conversion by binding in the active site. Inhibition of the enzyme occurs by removal and chelation of the metal ion required for catalytic activity, leaving an inactive apoenzyme. 1,10-Phenanthroline has been shown to mainly target zinc metallopeptidases and the inhibition of QC by 1,10-phenanthroline has been previously described [99]. EDTA has been shown under certain conditions to have an activating effect on QC catalysis and our data confirms that small amounts display an activating effect. It has previously been suggested that inhibition by phenanthroline is not due to metal chelation [94]. Also, in addition to being inhibited by 1,10-phenanthroline, *P. gingivalis* QC-catalyzed substrate cyclization was abolished in presence of dipicolinic acid, another inhibitor of metalloenzymes. Both chelators inhibited QC in a concentration and time-dependent manner, i.e. initial activity that was already

inhibited was found to be further reduced after prolonged incubation with the compounds (Fig. 8). However, EDTA did not show remarkable inhibition of *P. gingivalis* QC until the concentration was increased almost to 2.0 M. *P. gingivalis* QC was almost completely inactivated addition of 5 mM 1,10-phenanthroline. Schilling et al. have previously shown that repeated dialysis with chelator-free buffer, human QC activity was partially reactivated up to 50–60% but only in the presence of EDTA [94].

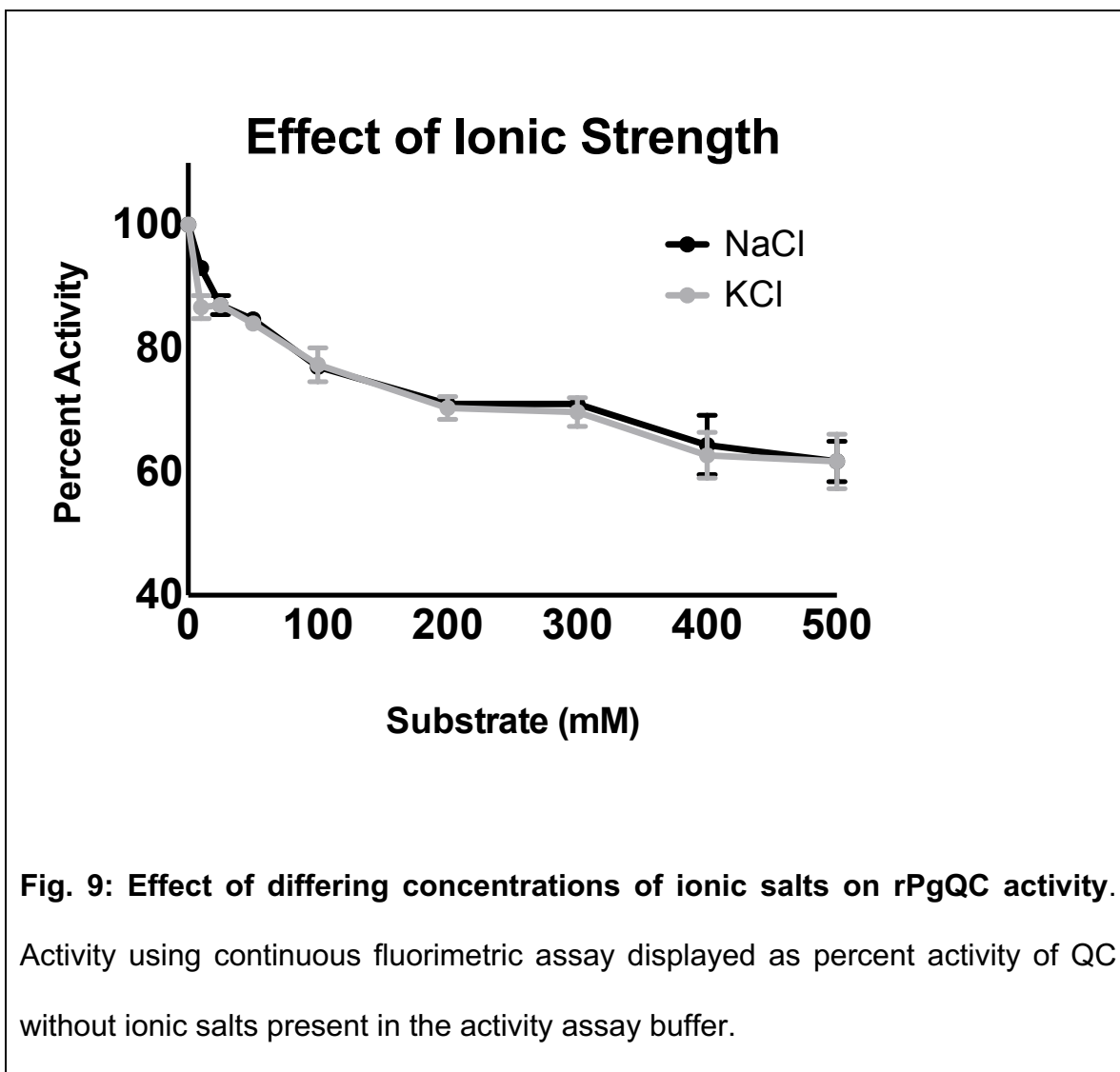
	Residual activity (%)		
	0.1 mM	1 mM	10 mM
Imidazole	84	42	19
Cysteamine	39	11	1
DTT	85	72	57
Gluthathione	97	85	9
L-Cysteine	89	75	23

Table 5. Attenuation of rPgQC activity by reducing agents and imidazole.

Reactions were carried out at 30 °C in 0.06 M acetic acid, 0.06 M Mes, and 0.12 M Tris adjusted to the respective pH by the addition of NaOH or HCl. Data shown as residual activity set as 100% for given reaction without inhibitor. Data points are averaged triplicates.



To confirm effect of ionic strength on the activity of rPgQC, activity assay buffer was supplemented with differing concentrations of NaCl and KCl. rPgQC activity saw a sharp drop in activity with the addition of ion salts, but then activity tapered off to around 50% activity as the concentration of ion salts increased dramatically. (Fig. 9)



Sensitivity of the QC reaction to metal ions was also probed. Using the continuous fluorimetric assay, a reaction mixture was pre-incubated with the respective ion salt. Out of tested divalent cations only Cu^{2+} exerted strong inhibitory activity (Table 6). Other metal ions had only slight effect only at 10 mM concentration in the reaction mixture. Interestingly but not surprisingly, increasing Zn^{2+}

concentrations within the QC assays (0.1 mM and higher) considerably reduce QC activity, and this has been observed in previous studies [94, 123].

<u>Residual activity (%)</u>			
	<u>0.1 mM</u>	<u>1 mM</u>	<u>10 mM</u>
MgCl ₂	88	83	71
CaCl ₂	93	82	61
CuSO ₄	2	0	0
BaCl ₂	93	82	61
MnCl ₂	90	63	13
ZnCl ₂	6	2	0
FeCl ₃	88	77	18
CuCl ₂	1	0	0

Table 6: Residual activity of rPgQC in the presence of competing metal ions.

Given as percent activity of rPgQC standard. Performed on 96-well plate in triplicate, experiment repeated in triplicate. Values represent mean of the different results.

Pyroglutamate is present in signal peptidase I substrates

In order to experimentally demonstrate pyroglutamate at the amino-terminus of SPI substrates, previously determined mass spectrometry data was re-analyzed for *P. gingivalis* outer membrane vesicles [73, 136]. Outer membrane vesicles (OMVs) are continuously shed. Their vesicle lumen (VL), vesicle membrane (VM) and vesicle surface (VS) fractions contain proteins that are derived from the periplasm, the outer membrane, and extracellular proteins anchored to the outer membrane surface, respectively [148]. Pyroglutamate was inferred from the mass of the identified peptide, which is 17 Da less than what the unmodified peptide, and also by the fragmentation (MS/MS) pattern of the peptide. The MS/MS spectra of these peptides indicate that the -17 Da modification is present near the N-terminus of each peptide, most consistent with pyroglutamate formation. Altogether 27 proteins, all putative SPI substrates, with N-terminal pyroglutamate were identified. Interestingly, no semi-tryptic peptides with N-terminal glutamine were found in the entire *P. gingivalis* dataset, suggesting widespread pyroglutamate formation, despite the incomplete evidence for the complete set.

In order to further confirm this conclusion, we compared sequences around the cyclization site (and thus the SPI cleavage site) for proteins that were experimentally identified, had a glutamine after the predicted SPI cleavage site, and for which evidence for pyroglutamate formation was either available or not.

The region upstream of the SPI cleavage site, normally not expected to influence QC, was included in the comparison in case SPI and QC may act together and QC preferences may be influenced by SPI preferences. However, we did not detect clear differences in the sequence logos of the two groups of proteins on either side of the critical Q residue, further supporting the conclusion that QC acts broadly and is not limited in its activity by specificity for residues adjacent to the substrate glutamine residue (Table 7). Also noted is the fact that proteins with experimental evidence for pyroglutamate formation at the N-terminus were present in all compartments of outer membrane vesicles, this would subsequently stand against a role in partitioning proteins between VL, VM or VS of OMVs or the equivalent periplasmic space, outer membrane and outer membrane surface that these proteins stem from (Table 7).

	<i>P. gingivalis</i>			<i>T. forsythia</i>		
	VL	VM	VS	VL	VM	VS
Total	27	79	30	61	172	27
Q	19	36	24	n.d.	n.d.	n.d.
SIGNALP = Y	19	46	20	40	84	15
SIGNALP = Y&Q	10	19	16	27	31	12
pGlu detected	7	11	6	6	9	8

Table 7: Q-value. Proteins from these compartments stem from the periplasm, the outer membrane, and the outer membrane surface, respectively. The row “Total” indicates the number of localized proteins, the row “Q” the number of proteins with a Q exposed by SPI signal peptide cleavage (according to a prior manual annotation, not focused on pyroglutamate formation), the row “SIGNALP = Y” the number of proteins with signal peptide, and the row “SIGNALP = Y&Q” the number of such proteins exposing a glutamine after signal peptide cleavage. The row “pGlu detected” identifies the number of proteins with experimentally verified pyroglutamate. In very few instances, a pyroglutamate was detected in a protein not predicted to expose a glutamine after signal peptide cleavage due an erroneous SIGNALP prediction.

Q downstream of the SPI cleavage site affects RgpA, but not RgpB and Kgp secretion

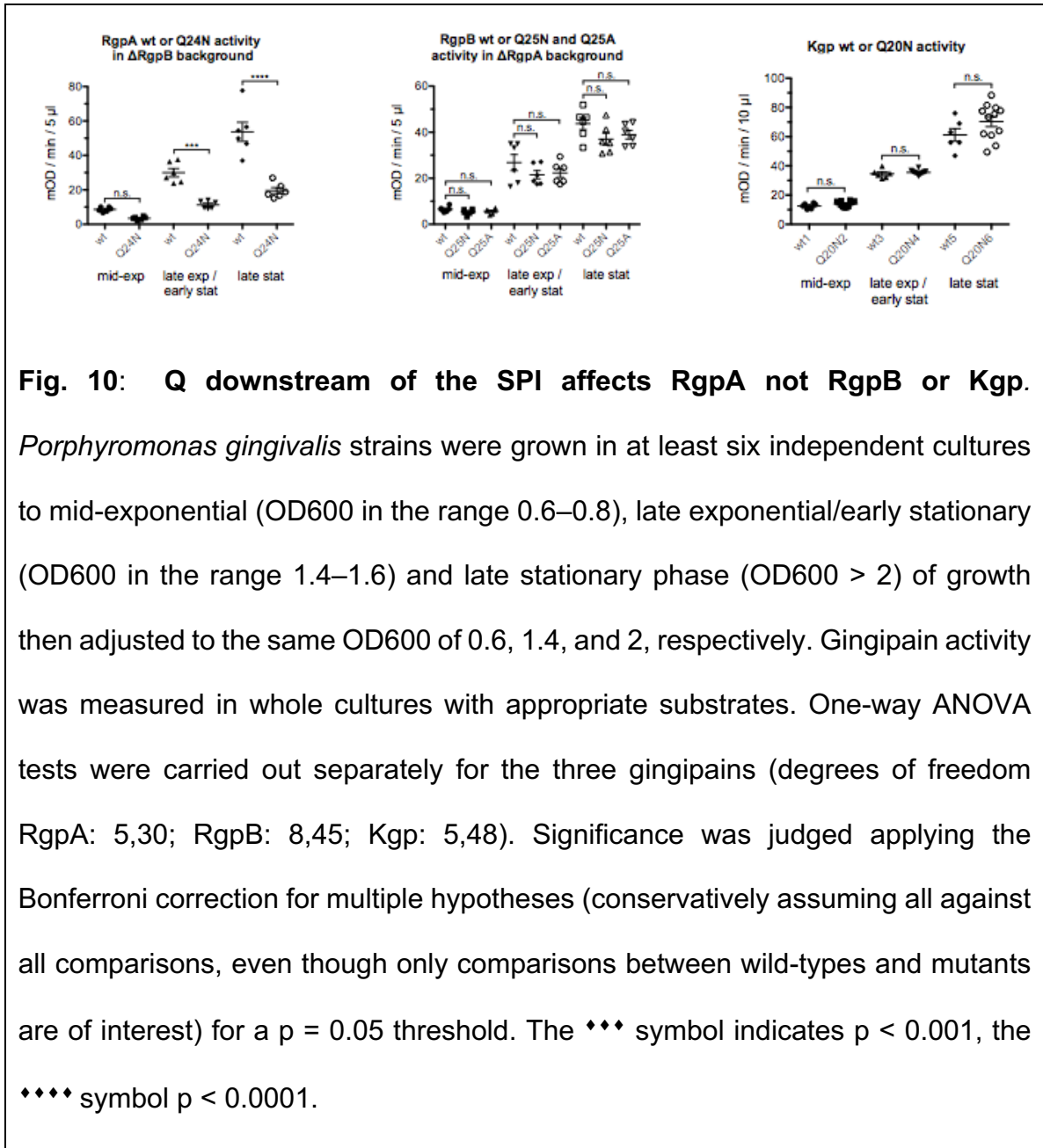
In order to confirm that pyroglutamate formation does not affect secretion, we needed a model system in which pyroglutamate formation does not influence protein stability by controlling resilience against aminopeptidases. Gingipains RgpA, RgpB and Kgp, the major proteolytic virulence factors of *P. gingivalis*, are good model systems in this respect. The proteins are initially expressed as preproteins, and their type I signal peptides are then cleaved upon import into the periplasm, exposing N-terminal glutamine residues. The CTD-domain containing proteins are then exported further by the type IX secretion system (T9SS). Upon secretion from the periplasm to the outer membrane surface, the pro-regions are rapidly degraded, leaving only the mature forms that no longer contain the expected pyroglutamate N-terminal residue. This is an asset for comparing protein activity independent of issues of protein stability, but it unfortunately also prevents detection of the pyroglutamylation of the pro-region in wild-type *P. gingivalis* strains. Nevertheless, we expect pyroglutamate formation based on its widespread occurrence (see above), and also because proRgpB is blocked for Edman degradation in a type IX secretion (T9SS) mutant that retains non-degraded proRgpB in the periplasm.

We used homologous recombination to construct *P. gingivalis* W83 strains expressing RgpAQ24N, RgpBQ25N, RgpBQ25A and KgpQ20N, in Δ RgpB,

Δ RgpA and wild-type backgrounds, respectively. Due to overlapping RgpA and RgpB specificities (both enzymes cleave after arginine residues), RgpA activities had to be compared in Δ RgpB background, and *vice versa*, whereas Kgp activities could be compared in a wild-type background. Mutation of the RgpA, RgpB or Kgp glutamine after the SPI cleavage site did not alter *P. gingivalis* growth or the extracellular activity of prolyl tripeptidyl peptidase secreted by *P. gingivalis* independent of T9SS. Gingipain activity was assayed in full cultures and the cell-free culture medium from cultures grown to the mid-exponential ($OD_{600\text{ nm}} = 0.6-0.8$), late exponential/early stationary ($OD_{600\text{ nm}} = 1.2-1.4$) and stationary ($OD_{600\text{ nm}} > 2.0$) phase of growth. We assayed either total extracellular activity, or separately the activities associated with the outer membrane surface and with the culture medium. In all cases, activities increased strongly over time from mid-exponential to late stationary cultures. Mutation of the Q after the SPI cleavage site however, had surprisingly variable effects on the different gingipains.

The Q24N mutation in RgpA reduced overall activity several-fold, whereas the equivalent substitution Q25N (and also Q25A) in RgpB and Q20N in Kgp lacked significant effect, irrespective of whether cells were assayed in mid-exponential, late exponential/early stationary or late stationary phase (Fig. 10).

For all three gingipains, most of the activity was cell-associated, with only a minor contribution from protein in the medium. For RgpA, the Q24N decreased cell



associated activity several fold, in all phases of growth. Activity in the medium was also significantly reduced in late stationary phase, the only growth stage with more than a marginal contribution from protein in the medium to the overall activity. In contrast, for RgpB, both the Q25N (and also Q25A) mutations altered the activity

associated with cells and in the medium at most insignificantly. There was also no redistribution of activity between cells and medium. For Kgp, the Q20N substitution had an unexpected effect. Although the overall activity was not significantly altered, Q substitution in Kgp increased activity in the medium at the expense of activity associated with cells, especially in mid-exponential phase, and to a lesser extent also in late exponential/early stationary phase.

We suspect that the diverse effects of Q substitution must be related to complicated posttranslational processing of Kgp and RgpA leading to an assembly of large multidomain complexes of the catalytic and hemagglutinin-adhesion domains derived from initial polyproteins anchored into the OM via A-LPS [149] rather than *per se* translocation of the OM.

QC is Essential for *P. gingivalis* Survival

Creation of non-polar QC knock-out strains in *P. gingivalis* was an untenable goal due to apparent lethality of absence of QC activity. *P. gingivalis* QC (PG_2157) lies within an operon containing genes PG_2157, PG_2156, and a HemG (PG_2158), and in initial attempts downstream effects were present in the gene replacement (Fig. 11). t. Subsequently we attempted construction of non-polar knock out strains, without disrupting the operon but it was evident that gene PG1885 is essential for survival of *P. gingivalis* bacteria. Partial success was

achieved with only one survivable mutant in which erythromycin was successfully inserted between PG_2157 and PG_2158.

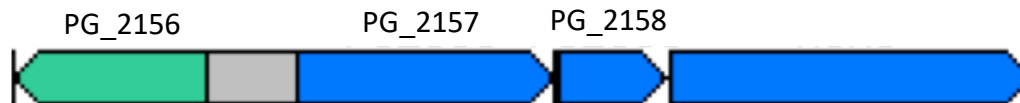


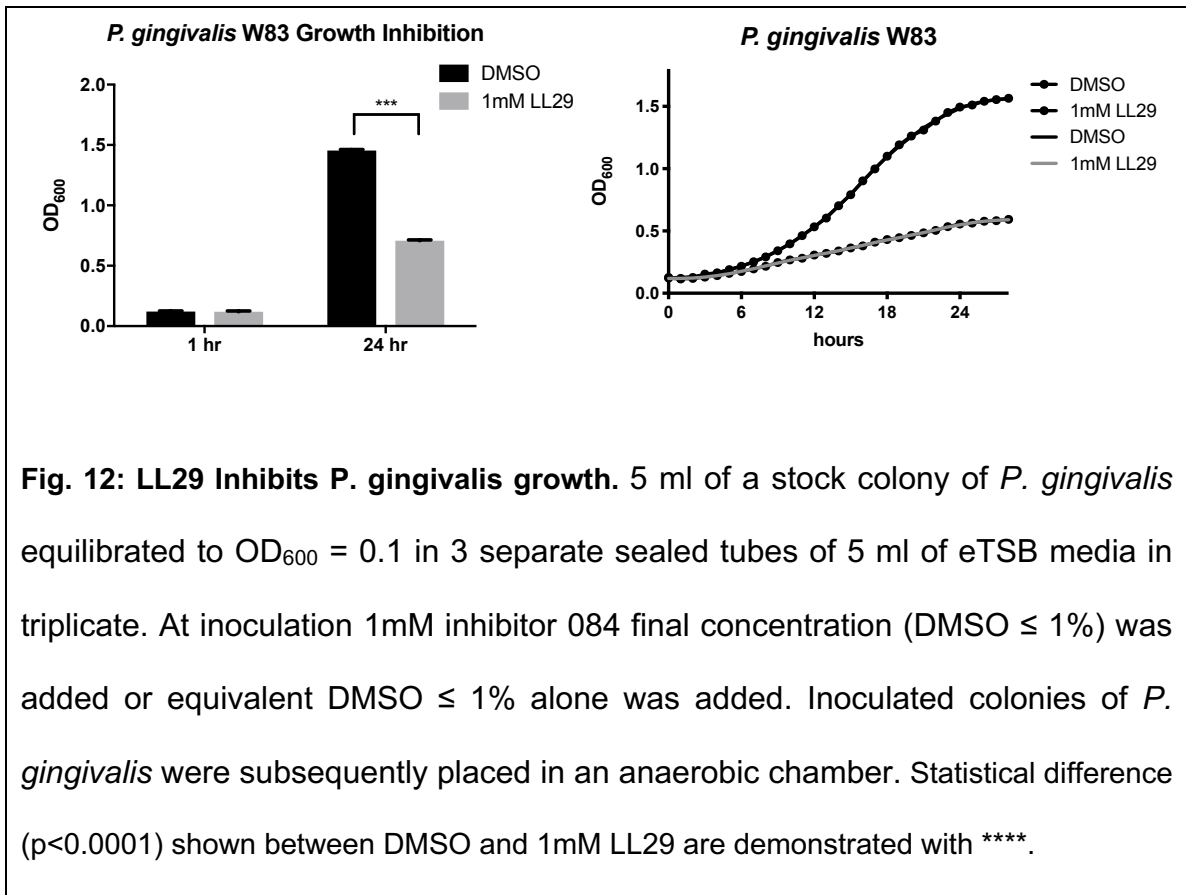
Fig. 11: Structural Schematic of the *P. gingivalis* operon containing QC. Gene coding sequence PG_2157 (QYT). PgQC lies just prior to PG_2156 and PG_2158 and non-polar disruption of PG_2157 was lethal.

Following these revelations, we shifted focus into examining and manipulating the possible QC targets that were identified during the SignalP QC distribution data.

***P. gingivalis* growth attenuation by PgQC Inhibition**

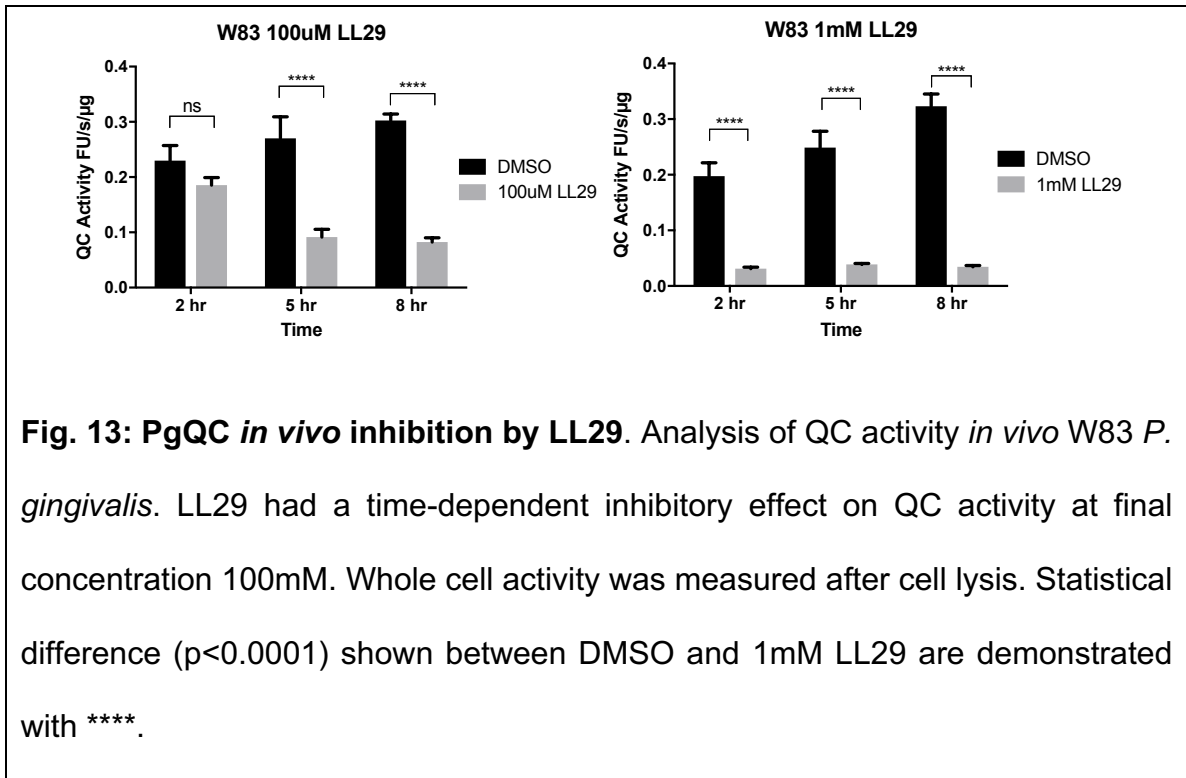
After assessing the effects of non-specific inhibitors of QC activity both *in vitro* and *in vivo*, specific inhibitors were produced to experimentally determine the effects of reduced PgQC activity on bacterial growth. With the assistance and cooperation of Probiodrug in Germany, banks of specific inhibitors were screened against purified rPgQC. Promising candidates were then analyzed for inhibition on QC

activity. The initial inhibitor was LL29. Inhibitor LL29 was dissolved in DMSO into 100mM concentration and incubated with fresh *P. gingivalis* liquid culture. 1.5ml of liquid culture of *P. gingivalis* were lysed, and remaining LL29 inhibitor was washed with PBS and QC activity was recorded using fluorimetric assay. In these cell lysates cultures that were administered 100mM LL29 showed a time-dependent competitive inhibition of PgQC. In addition to the in vitro effects of LL29 on PgQC, corresponding 1.5 mL cultures of early-log phase *P. gingivalis* were incubated overnight to examine the inhibitors' effect on *P. gingivalis* growth. After 24-hour incubation in anaerobic chamber, the OD₆₀₀ of cultures was analyzed. LL29 inhibitor incubated cultures showed a decrease in absorbance equivalent to 33% cell density decrease. Initially we suspected that the cell permeability may be a complicating factor or extracellular inhibitor could be degraded by cell factors. To effectively rule out inhibitor penetration into bacteria cells, these experiments were repeated in triplicates but concentrations of LL29 were increased 10 fold to 1mM and compared to initial 100mM concentration. (Fig. 12)



What is striking is the group with 1mM LL29 showed a remarkable decrease in QC activity along with a 50% decrease in total liquid culture density (Fig 12). 24-hour growth curves were plotted to demonstrate LL29's effect over time (Fig. 12B). Absorbance readings were taken at 1-hour intervals over a 28-hour period and plotted to display accurate growth curves. These showed that the cultures with 1mM LL29 only reached an absorbance of less than half of the control group (DMSO alone). RgpA-null strain cultures were pre-incubated with LL29, pelleted, washed three times with PBS and then resuspended in fresh eTSB media to

removed trace amounts of excess LL29 not taken up by the bacteria. This eliminated excess inhibitor from the reaction. 100mM LL29 demonstrated time-dependent inhibition of W83 *in vivo* QC activity. This inhibition was more pronounced at 1mM concentration (Fig. 13).



Samples were then taken at 2, 5, and 8-hour marks and whole cell gingipain activity assays were completed. Using the data stated above, further screening of potential specific inhibitor produced 5 additional possible candidates. Inhibitors: 019, 071, 073, 101, and 084 were roughly screened using *in vitro* PgQC assays. Each inhibitor showed significant attenuation of PgQC activity but only 084 completely obliterated QC activity (Fig. 14). Previously, each respective inhibitor was incubated within the reaction mixture prior to initiation of the assay. In the case of

084, we wanted to determine if the inhibitor had a bacteriocidal or bacteriostatic effect, so the growth curve was repeated with addition of 1mM 084 at mid-logarithmic bacterial growth (Fig. 14F) After addition of 084, bacterial cell density decreased slowly up to 24 hrs after which it remained static. This suggests some mixed bacteriostatic/bacteriocidal killing of *P. gingivalis* after addition of inhibitor 084 at 1mM final concentration.

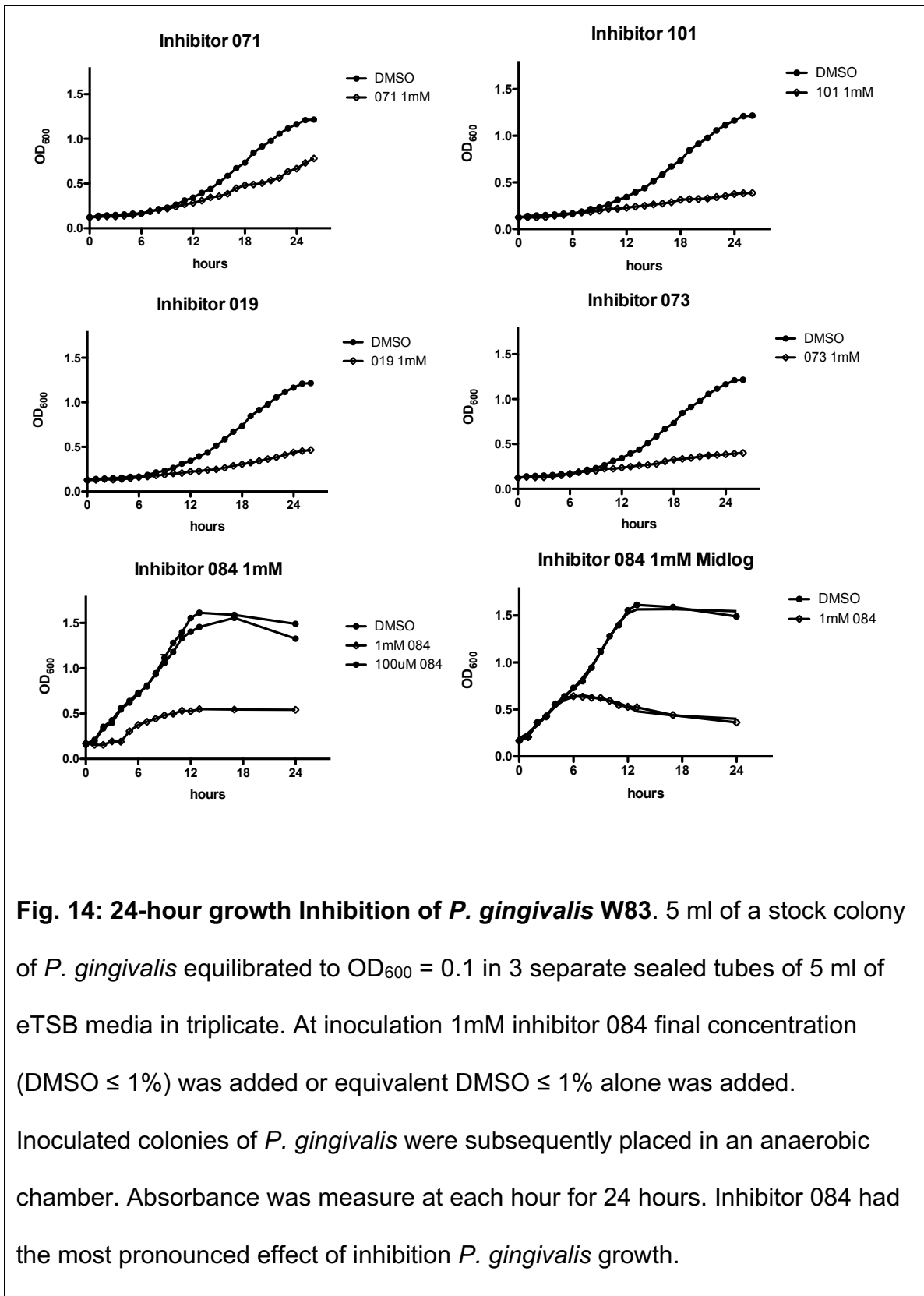


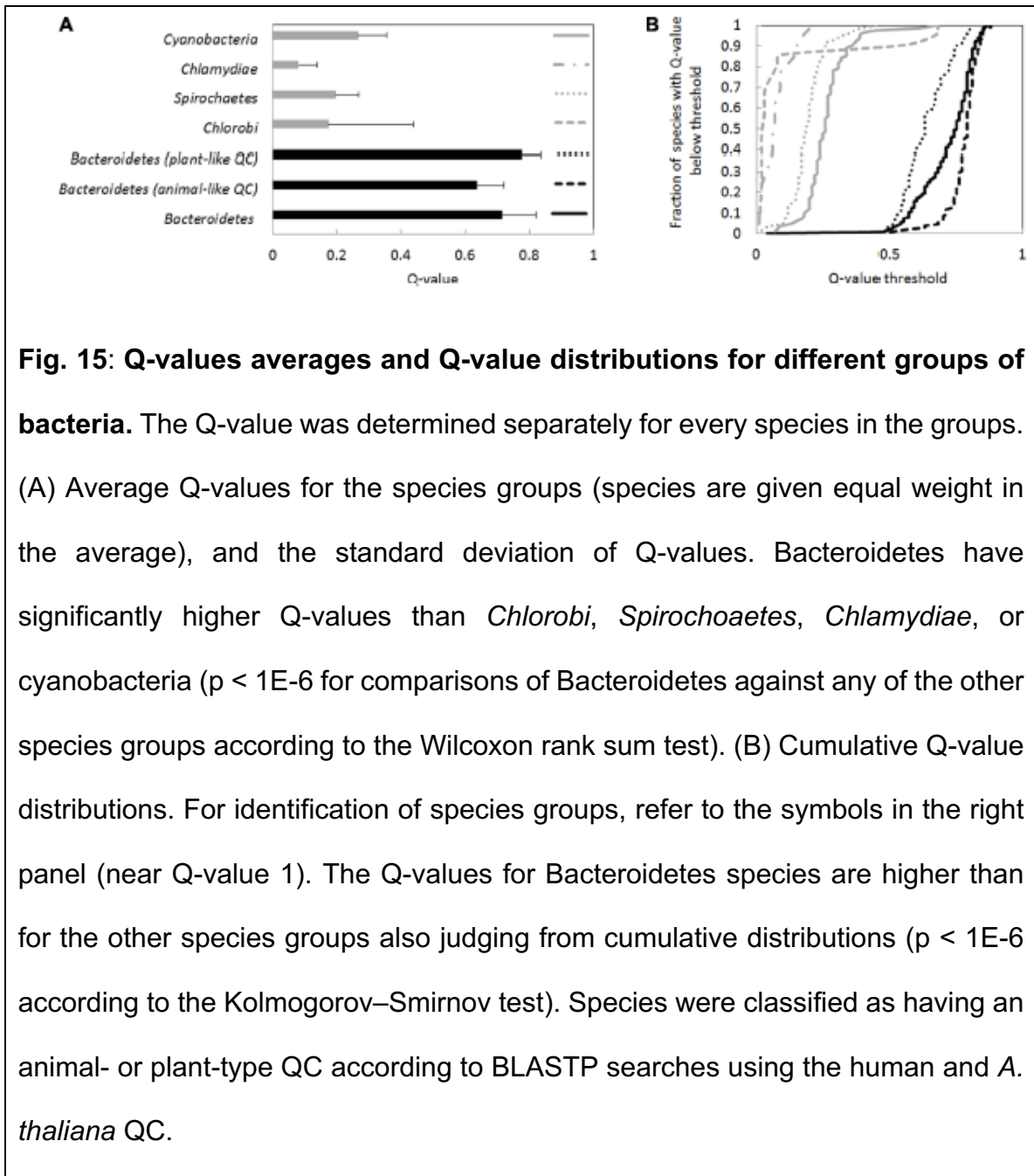
Fig. 14: 24-hour growth Inhibition of *P. gingivalis* W83. 5 ml of a stock colony of *P. gingivalis* equilibrated to OD₆₀₀ = 0.1 in 3 separate sealed tubes of 5 ml of eTSB media in triplicate. At inoculation 1mM inhibitor 084 final concentration (DMSO ≤ 1%) was added or equivalent DMSO ≤ 1% alone was added. Inoculated colonies of *P. gingivalis* were subsequently placed in an anaerobic chamber. Absorbance was measure at each hour for 24 hours. Inhibitor 084 had the most pronounced effect of inhibition *P. gingivalis* growth.

High Q-values are typical for *Bacteroidetes* species, but not related phyla

In the following, we call the fraction of signal peptidase I substrates that have a glutamine immediately downstream of the SPI cleavage site the Q-value. The high Q-value is not unique for *P. gingivalis* but is shared with other bacterial species. LipoP corrected SignalP predictions for various *Porphyromonas* species suggest Q-values between 59% (for *P. somerae*) and 77% (for *P. macacae*). Manual inspection of automatic prediction suggested that even the high Q enrichment values are still underestimated due to the mis-prediction of some signal peptide cleavage sites.

Porphyromonas species belong to *Bacteroidetes*, which in turn are placed in the FCB superphylum containing the *Fibrobacteres*, *Chlorobi*, and *Bacteroidetes*. In the *Bacteroidetes* group, 332 of 334 species (i.e. > 99%) had predicted Q-values above 48%. Averaged across species, the Q-value was 71%, with a standard deviation for the variation between species of around 10% percent (outliers included). The two low Q-value outlier species (*Bacteroides pectinophilus*, 4% and *Candidatus cloacimonas* 24%) had a suspiciously low number of predicted proteins with signal peptides (21 and 83, compared to typically 300 in this group), suggesting a possible problem with sequencing or annotation rather than a genuine difference. CELLO predictions for *T. forsythia* confirm the conclusion for *P. gingivalis* that the enrichment of glutamine residues directly after the SPI

cleavage site is not specific for proteins of a particular cellular compartment (Table 3). Across the entire FCB superphylum, Q-values were not consistently high. For most sequenced *Chlorobi* species, the predicted Q-value was below 9%. Three outliers were found in this group in little characterized bacteria (annotated as *Chloroherpeton thalassium*, Q-value 55%, *Chlorobi* bacterium, Q-value 63% and *Chlorobium* sp., Q-value 67%). Outside the *Bacteroidetes* and *Chlorobi*, a continuum of Q-values was found, ranging from 2% (*Chlorobaculum parvum*) to 77% (*Ignavibacterium album*), with no obvious pattern.



We also determined the cumulative Q-value distribution for selected bacterial phyla (Fig. 15), thought to be relatively closely related to *Bacteroidetes* [150]. Predicted Q-values for *Chlamydiae* and *Spirochaetes* species were typically below 20% and thus much lower than in *Bacteroidetes*. Cyanobacterial species typically also had

lower Q-values. However, in a small fraction of cyanobacterial species (~5%), Q-values were not much lower than those of *Bacteroidetes*. High Q-values were for example found for *Scytonema millei* (40%), *Leptolyngbya valderiana* (45%), *Hassallia byssoidea* (61%), and *Aphanocapsa montana* (67%) (Fig 15).

***Bacteroidetes* have orthologues of animal and plant QCs**

We searched complete bacterial proteomes in UNIPROT for orthologues of animal- and plant-type QCs. In a first step, we used the prototypical human and *A. thaliana* QC sequences as queries. In a set of 1878 proteomes, we found 602 animal-type QCs, among them 402 (67%) in *Bacteroidetes*. We also identified 991 plant-type QCs, among them 401 (40%) in *Bacteroidetes*. As *Bacteroidetes* account for less than 10% of the proteome data (and even less in the redundant set), it is clear that QCs, particularly of the animal-type, are enriched in the *Bacteroidetes*. Orthologues of animal- and plant-type QCs tended to segregate according to phylogeny. Animal-type QCs were typically found in *Bacteroidia*, plant-type QCs in *Flavobacteriia*. As the number of candidate QCs was smaller than the number of proteomes, we attempted to enlarge the set of candidate QCs by carrying out BLASTP queries with representative sequences from *Bacteroidia* and *Flavobacteriia*, the two largest groups within the *Bacteroidetes*. Starting from these sequences, and correcting for species duplicates, we identified 574 *Bacteroidetes* species containing animal-type and 507 *Bacteroidetes* species containing plant-type QC enzymes, but only 63 species containing both types of

enzymes (E-value threshold 1E-4), compared to 1540 species in the duplication corrected proteome dataset.

We also attempted iterated searches, using representatives of CD-HIT identified sequence clusters [151] to initiate additional searches. With this procedure, still more putative QCs were identified, but the concentration of hits in the *Bacteroidetes* phylum was reduced, likely because the set of putative QCs became contaminated by peptidases. Despite this complication, we can conclude from the simpler BLASTP searches that most and perhaps even all *Bacteroidetes* species have enzymes that could be suitable for glutamine cyclization. In the following, we focus on the candidate QC enzymes that can be demonstrated in a single BLASTP step with tight E-value threshold to be orthologous to the prototypical animal- or plant QC enzymes.

The orthologues of animal and plant-like QCs in *Bacteroidetes* have intact active sites

In order to assess the chances that the animal- and plant-type QCs in bacteria were active, we checked alignments for the presence of key active site residues. The prototypical animal QC is the human enzyme, hsQC. Its active site is built from E201 (involved in proton shuttling), D159, E202 (involved in binding the active site Zn²⁺ ion), and D248 (involved in both). In the *Bacteroidetes* orthologues of human QC, D159, E201 and D248 are highly conserved (>98%). In contrast, E202 is

conserved only in 9% of *Bacteroidetes* orthologues, and replaced by an aspartate residue almost all remaining cases (exceptions <1%). As aspartate and glutamate can both serve as Zn²⁺ ligands, we suspect that this substitution may not compromise activity, or may even be required to accommodate slight changes in the overall protein structure compared to HsQC. This conclusion is supported by the observation that an aspartate is also present in the 202 position in the PgQC enzyme, which we have already shown to be an active QC enzyme.

The prototypical plant QC is the enzyme from *C. papaya*, CpQC. Its active site is not as well understood as the active site of hsQC, but it is thought that E69, N155 (probably involved in proton shuttling) and N155, K225 and Q24 (probably involved in stabilizing the oxyanion intermediate) play a role in catalysis. Among the *Bacteroidetes* orthologues, E69, N155 and K225 are strictly conserved. In contrast, Q24 was conserved only in 81% of cases, and replaced by a glutamate in the remaining cases. The same substitution occurs in many plant enzymes, and also in the experimentally studied bacterial *Xanthomonas campestris* QC (XcQC). In this special case, the (natural) glutamate variant is still active, albeit an order of magnitude less so than the engineered glutamine variant [91], suggesting that both glutamine and glutamate in the active site are compatible with activity, although not necessarily at the same level.

We conclude from this analysis that *Bacteroidetes* orthologues of animal and plant QCs are likely to be active enzymes. This is directly suggestive of QC activity plant

QC orthologues, and compatible with either QC or aminopeptidase activity for animal QC orthologues. Classification of the enzymes as lipoproteins (like PgQC) could strengthen the case for QC activity.

Most *Bacteroidetes* orthologues of animal and plant QCs are predicted lipoproteins

Among 401 orthologues of human QC in *Bacteroidetes*, 323 (~80%) were predicted lipoproteins, 59 (~15%) were predicted SPI substrates (~15%), and the remaining 19 (~5%) were predicted to be cytoplasmic. As orthologues of human QC are highly enriched in *Bacteroidetes*, relatively few were found in species not belonging to the *Bacteroidetes*. Among these, the fraction of predicted lipoproteins was much smaller. Only 38 (~34%) enzymes were predicted to be lipoproteins, 40 (~36%) were classified as SPI substrates, and remaining 34 (~30%) as cytosolic proteins.

Among 430 orthologues of *A. thaliana* QC in *Bacteroidetes*, 376 were (~87%) computationally classified as lipoproteins, 20 (~5%) as SPI substrates, and 34 (~8%) as cytoplasmic proteins. The predominance of predicted lipoproteins among plant-type QCs was much less pronounced when bacterial homologues of plant QC in general were considered. Among the 1000 bacterial proteins most similar to *A. thaliana* QC, predictions classified 475 (~48%) as lipoproteins, 338 (34%) as SPI substrates, and 175 (18%) as cytosolic proteins.

Sensitivity (true positive rate, recall) of the LipoP algorithm for gram-negative bacteria has been reported to be around 90% [140]. The fraction of bacterial QCs predicted to be lipoproteins in non-*Bacteroidetes* species is much smaller, suggesting that not all are lipoproteins. In *Bacteroidetes*, the fraction of QC proteins predicted as lipoproteins comes close to the predicted sensitivity of the prediction algorithm. Thus, it appears likely that most if not all QCs in *Bacteroidetes* are lipoproteins, like the prototypical PgQC from *P. gingivalis*.

Proteomic datasets confirm glutamine cyclization in several *Bacteroidetes* species

In order to confirm widespread pyroglutamyl formation in *Bacteroidetes*, and not only *P. gingivalis*, we analyzed additional data from previously reported proteomic studies [73, 134-137]. In addition to the already discussed 27 proteins from *P. gingivalis*, the collated data identify 27 proteins in *Tannerella forsythia*, 13 in *Parabacteroides distasonis*, 8 in *Prevotella intermedia* and 7 in *Cytophaga hutchinsonii* with N-terminal pyroglutamate residue. N-terminal residues other than pyroglutamate were rare, as predicted from the bioinformatic studies.

Pyroglutamate was not detected at the amino-terminus of all SPI substrates that are predicted to expose an N-terminal glutamine residue after SPI cleavage, most likely due to incomplete coverage and not due to selective pyroglutamate

formation. As already reported for the *P. gingivalis* proteins, semi-tryptic peptides were never found to start with glutamine, even though internal tryptic peptides could be identified with N-terminal glutamine in both modified and unmodified states. Other circumstantial evidence also supports widespread rather than selective glutamine cyclization. We focused in particular on the *T. forsythia* data, which contained pyroglutamate evidence for the largest number of proteins in one species. Experimentally detected proteins (by any peptide, not necessarily a semitryptic peptide) with glutamine after the SPI site were partitioned into proteins with and without evidence for glutamine cyclization (Figure 16). As already reported for *P. gingivalis*, amino acids around the Q were similar in the two groups, supporting broad QC specificity.

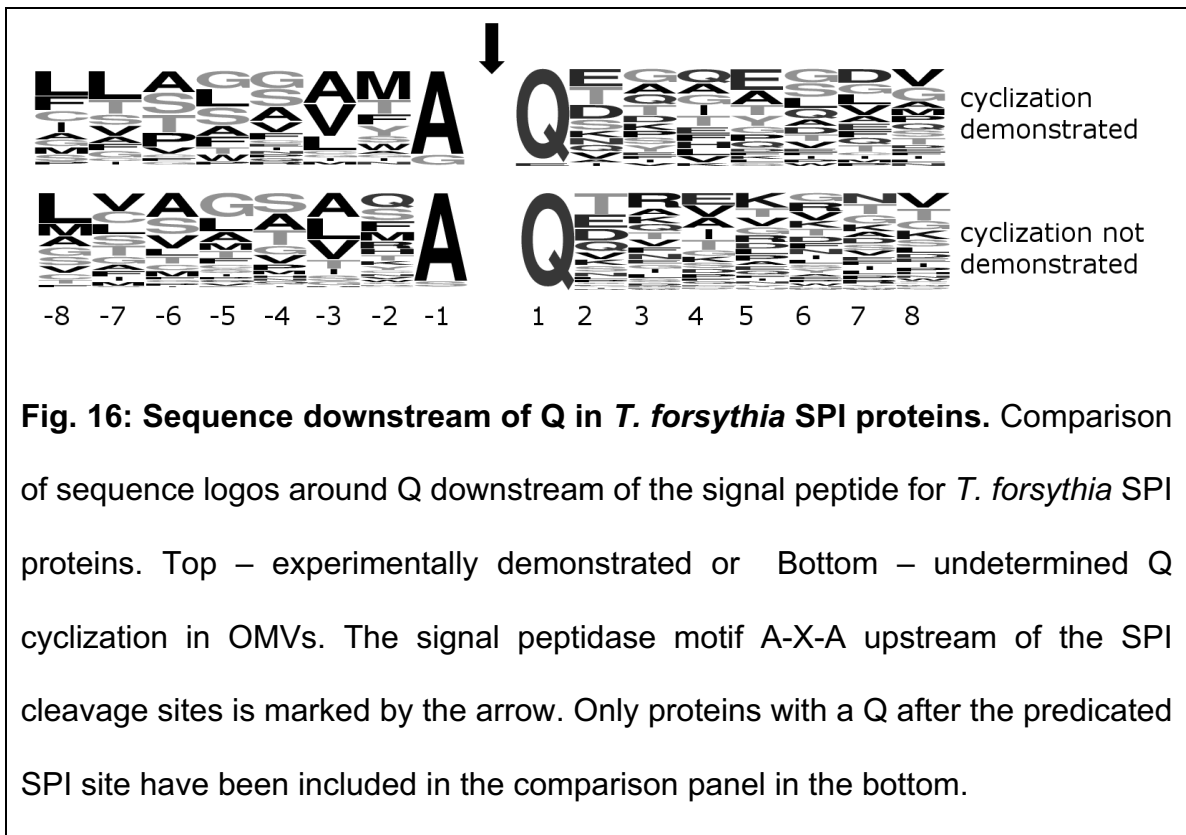
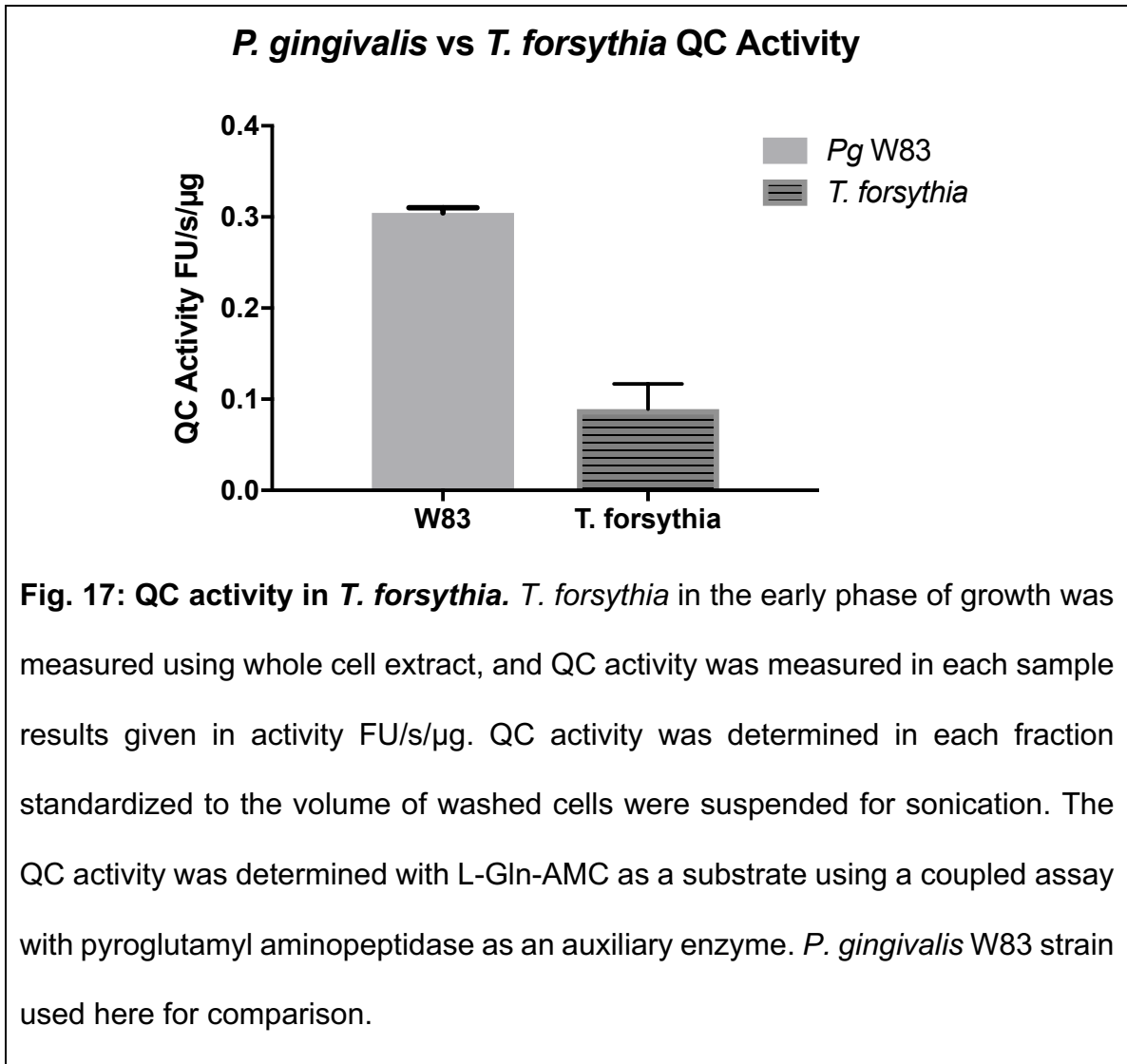


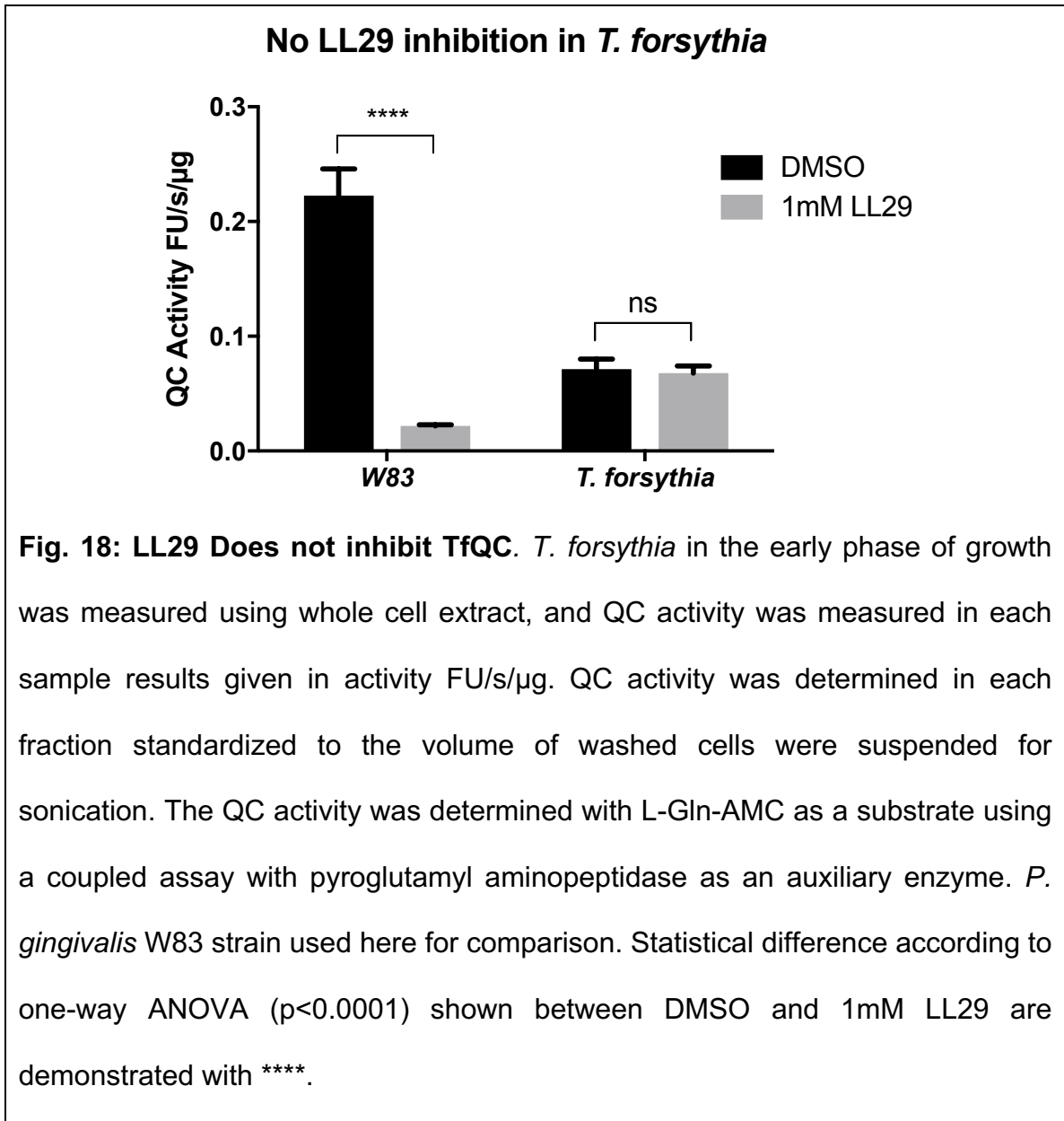
Fig. 16: Sequence downstream of Q in *T. forsythia* SPI proteins. Comparison of sequence logos around Q downstream of the signal peptide for *T. forsythia* SPI proteins. Top – experimentally demonstrated or Bottom – undetermined Q cyclization in OMVs. The signal peptidase motif A-X-A upstream of the SPI cleavage sites is marked by the arrow. Only proteins with a Q after the predicated SPI site have been included in the comparison panel in the bottom.

In addition, QC activity was detectable in *T. forsythia* using the previous method for continuous fluorimetric QC activity in *P. gingivalis* (Fig 17).



Following this experimentally measured QC activity of a *Bacteriodes* sp. Other than *P. gingivalis*, we decided to test the specificity of LL29 against the *T. forsythia* QC. LL29 demonstrated no inhibition of QC activity *in vivo* at any time point in *T.*

forisythia (Fig 18). This could be easily explained by substrate preference or variability in the active site structural motifs.



Pyroglutamate detection is not consistent for paralogue families in a single species. Pyroglutamate detection for a protein of a given bacterial species is also

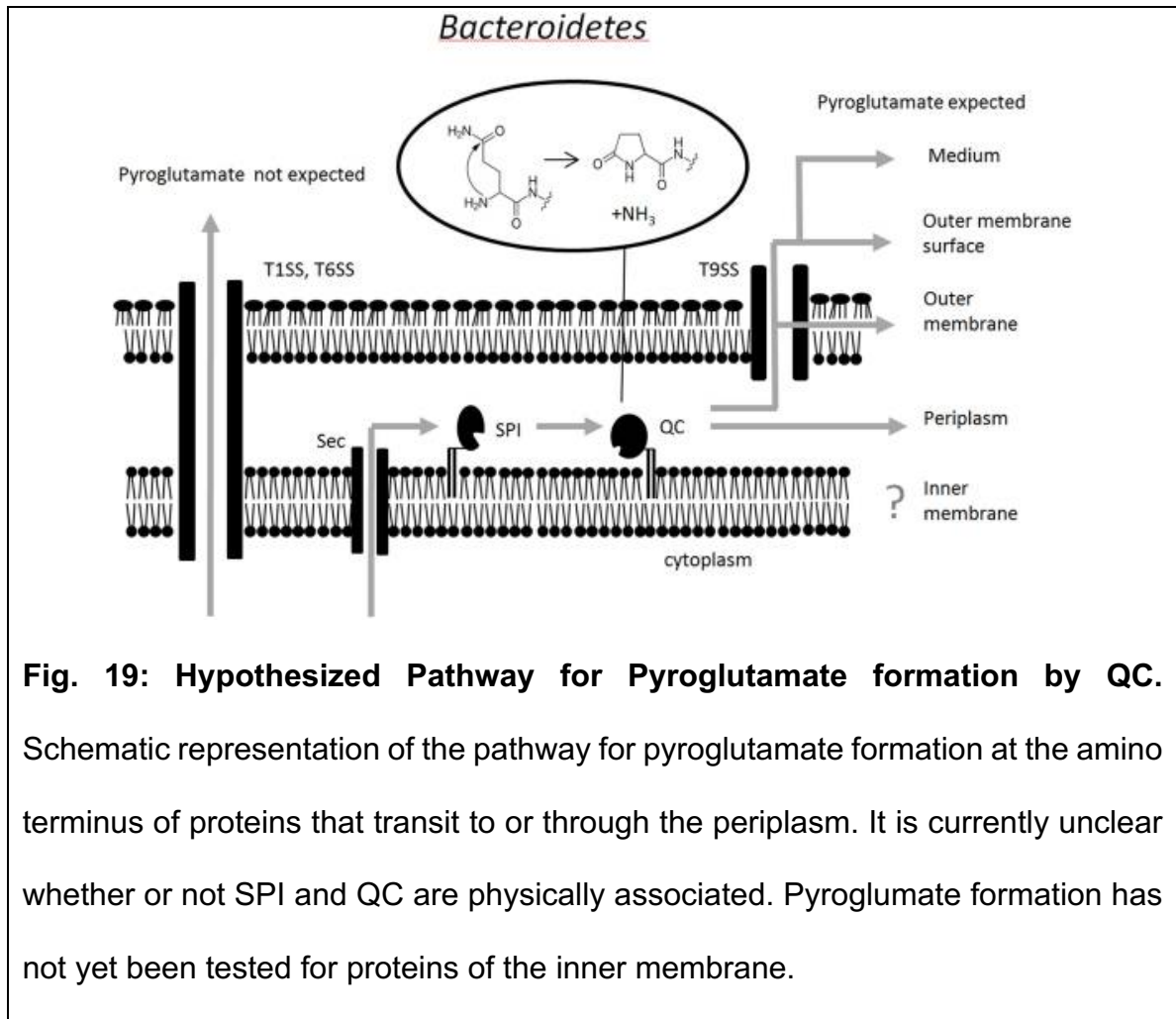
not predictive for the orthologue in another species. In a first step, we used BLASTP (E-value threshold 10^{-9}) to identify orthologous proteins in *T. forsythia* and *P. gingivalis* with experimentally verified localization. Only unique pairs were used, and proteins with more than one paralogue in either species were excluded. Among the 41 pairs, 9 and 3 were found to have a pyroglutamate at the N-terminal end. Based on a random association alone, one would then expect experimental pyroglutamate demonstration for both proteins of a pair in $(9 \times 3)/41 \sim 0.7$ cases. In fact, one such case was observed.

Together, the above observations are consistent with general glutamine cyclization, partially masked by incomplete mass spectrometry coverage (for example, due to low expression of some proteins, or because semi-tryptic peptides are too short or too long for efficient mass spectrometry detection). As already seen for *P. gingivalis*, pyroglutamate formation was not characteristic for proteins of a particular compartment, as *T. forsythia* proteins with pyroglutamate were also found in the vesicle lumen, in vesicle membranes, and on the vesicle surface of OMVs, which represent periplasmic, integral OM and cell-surface associated proteins, respectively.

A model for pyroglutamate formation in proteins destined to the periplasm, the outer membrane, the outer membrane surface, or the medium

Together, this body of data suggest a model for *Bacteroidetes* SPI substrates that reside in or transit through the periplasm. Their signal peptides are cleaved by SPI,

a lipoprotein with active site on the periplasmic face of the inner membrane. Because of the enrichment of glutamine immediately downstream of the SPI cleavage site, this reaction typically exposes an amino-terminal glutamine residue. QC, another lipoprotein, also with active site on the periplasmic face of the inner membrane, is then ideally positioned to catalyze the cyclization of the glutamine residue to a pyroglutamate residue. The cooperation between SPI and QC is apparently efficient, suggesting either direct interaction or joint anchoring in lipid domains, which we have not yet tested. Pyroglutamate formation occurs for proteins that remain in the periplasm, as well as for proteins that are transported further into or through the outer membrane. We suggest the term “Q-rule” to describe the finding that glutamines are enriched after SPI cleavage sites, and that these glutamine residues are cyclized to form N-terminal pyroglutamate residues in proteins that are destined to the periplasm or beyond (Fig. 19).



Importance of the Q-rule pathway

The Q-rule pathway seems to be biologically important, not only judging by the number of proteins that are subject to the rule. *P. gingivalis* glutaminyl cyclase is present in both virulent and avirulent strains [152]. According to an unbiased large scale transposon mutagenesis screen [153], the enzyme is essential even in laboratory culture conditions when *P. gingivalis* is not pitted against a host immune system. It is currently unclear why the enzyme is essential. Our data speak against a role of the modification in protein sorting. Given the host-associated lifestyle of

many *Bacteroidetes* species, it is possible that glutaminyl cyclization protects secreted proteins against host aminopeptidases (excluding of course the host pyroglutamate aminopeptidases). However, this model does not explain why the Q-rule applies to SPI substrates that remain in the periplasm or why the glutaminyl cyclase is essential for *P. gingivalis* in culture conditions, unless *P. gingivalis* has become unable to do without the Q-rule and now needs pyroglutamate formation for protection against its own periplasmic proteases as well. Further lending credence to this theory is the lethality of QC knock-outs.

Future topics

One of the lingering questions remaining is how the QC and SPI interact withing the periplasmic space. It was not evaluated whether these are or are not in intimate contact or physically linked to one another, although their function is clearly linked. Another point of interest is perhaps although only downstream effects of gingipain secretion were evaluated in this project, *P. gingivalis* is fully capable of surviving without gingipain activity. Perhaps another essential protein or proteins processed through this system is blocked, thereby leading to cell death. Either way this system poses as a possible target for future studies and continued research.

REFERENCES

1. Armitage, G.C., *Development of a classification system for periodontal diseases and conditions*. Ann Periodontol, 1999. **4**(1): p. 1-6.
2. Armitage, G.C., *The complete periodontal examination*. Periodontol 2000, 2004. **34**: p. 22-33.
3. Armitage, G.C., *Periodontal diagnoses and classification of periodontal diseases*. Periodontol 2000, 2004. **34**: p. 9-21.
4. Eke, P.I., et al., *Prevalence of periodontitis in adults in the United States: 2009 and 2010*. J Dent Res, 2012. **91**(10): p. 914-20.
5. Preisser, J.S., et al., *A new way to estimate disease prevalence from random partial-mouth samples*. J Clin Periodontol, 2016.
6. Papapanou, P.N., *Epidemiology of periodontal diseases: an update*. J Int Acad Periodontol, 1999. **1**(4): p. 110-6.
7. Papapanou, P.N., *Periodontal diseases: epidemiology*. Ann Periodontol, 1996. **1**(1): p. 1-36.
8. Papapanou, P.N., J.L. Wennstrom, and K. Grondahl, *A 10-year retrospective study of periodontal disease progression*. J Clin Periodontol, 1989. **16**(7): p. 403-11.
9. Loe, H., A. Anerud, and H. Boysen, *The natural history of periodontal disease in man: prevalence, severity, and extent of gingival recession*. J Periodontol, 1992. **63**(6): p. 489-95.
10. Brown, L.J. and H. Loe, *Prevalence, extent, severity and progression of periodontal disease*. Periodontol 2000, 1993. **2**: p. 57-71.
11. Socransky, S.S., et al., *New concepts of destructive periodontal disease*. J Clin Periodontol, 1984. **11**(1): p. 21-32.
12. Jeffcoat, M.K. and M.S. Reddy, *Progression of probing attachment loss in adult periodontitis*. J Periodontol, 1991. **62**(3): p. 185-9.
13. Albandar, J.M. and E.M. Tinoco, *Global epidemiology of periodontal diseases in children and young persons*. Periodontol 2000, 2002. **29**: p. 153-76.
14. Tonetti, M.S., et al., *Principles in prevention of periodontal diseases: Consensus report of group 1 of the 11th European Workshop on Periodontology on effective prevention of periodontal and peri-implant diseases*. J Clin Periodontol, 2015. **42 Suppl 16**: p. S5-11.
15. Kortsik, C., A. Elmer, and I. Tamm, *Pleural effusion due to Histoplasma capsulatum and idiopathic CD4 lymphocytopenia*. Respiration, 2003. **70**(1): p. 118-22.
16. Smalley, J.W., et al., *Interactions of Porphyromonas gingivalis with oxyhaemoglobin and deoxyhaemoglobin*. Biochem J, 2002. **362**(Pt 1): p. 239-45.
17. Moore, W.E., et al., *Bacteriology of severe periodontitis in young adult humans*. Infect Immun, 1982. **38**(3): p. 1137-48.
18. Partridge, N.C., et al., *Regulation of prostaglandin production by osteoblast-rich calvarial cells*. Prostaglandins, 1985. **30**(3): p. 527-39.
19. Paster, B.J., et al., *The breadth of bacterial diversity in the human periodontal pocket and other oral sites*. Periodontol 2000, 2006. **42**: p. 80-7.

20. Socransky, S.S., et al., *Microbial complexes in subgingival plaque*. J Clin Periodontol, 1998. **25**(2): p. 134-44.
21. Lamont, R.J. and G. Hajishengallis, *Polymicrobial synergy and dysbiosis in inflammatory disease*. Trends Mol Med, 2015. **21**(3): p. 172-83.
22. Moore, W.E. and L.V. Moore, *The bacteria of periodontal diseases*. Periodontol 2000, 1994. **5**: p. 66-77.
23. Paster, B.J., et al., *Bacterial diversity in human subgingival plaque*. J Bacteriol, 2001. **183**(12): p. 3770-83.
24. Socransky, S.S. and A.D. Haffajee, *Periodontal microbial ecology*. Periodontol 2000, 2005. **38**: p. 135-87.
25. Haffajee, A.D., et al., *Subgingival microbiota in healthy, well-maintained elder and periodontitis subjects*. J Clin Periodontol, 1998. **25**(5): p. 346-53.
26. Socransky, S.S. and A.D. Haffajee, *Dental biofilms: difficult therapeutic targets*. Periodontol 2000, 2002. **28**: p. 12-55.
27. Haffajee, A.D. and S.S. Socransky, *Microbial etiological agents of destructive periodontal diseases*. Periodontol 2000, 1994. **5**: p. 78-111.
28. Sorkin, B.C. and R. Niederman, *Short chain carboxylic acids decrease human gingival keratinocyte proliferation and increase apoptosis and necrosis*. J Clin Periodontol, 1998. **25**(4): p. 311-5.
29. Wyss, C., *Dependence of proliferation of Bacteroides forsythus on exogenous N-acetylmuramic acid*. Infect Immun, 1989. **57**(6): p. 1757-9.
30. Teles, F.R., et al., *Early microbial succession in redeveloping dental biofilms in periodontal health and disease*. J Periodontal Res, 2012. **47**(1): p. 95-104.
31. Gmur, R., J.R. Strub, and B. Guggenheim, *Prevalence of Bacteroides forsythus and Bacteroides gingivalis in subgingival plaque of prosthodontically treated patients on short recall*. J Periodontal Res, 1989. **24**(2): p. 113-20.
32. Simonson, L.G., et al., *Bacterial synergy of Treponema denticola and Porphyromonas gingivalis in a multinational population*. Oral Microbiol Immunol, 1992. **7**(2): p. 111-2.
33. Hosaka, Y., et al., *Effect of initial therapy on dynamics of immunoglobulin G levels to some periodontopathic bacteria in serum and gingival crevicular fluid*. Bull Tokyo Dent Coll, 1994. **35**(4): p. 207-16.
34. Umeda, M., et al., *Microbial flora in the acute phase of periodontitis and the effect of local administration of minocycline*. J Periodontol, 1996. **67**(4): p. 422-7.
35. Ali, R.W., et al., *Detection of identical ribotypes of Porphyromonas gingivalis in patients residing in the United States, Sudan, Romania and Norway*. Oral Microbiol Immunol, 1997. **12**(2): p. 106-11.
36. Karunakaran, T., T. Madden, and H. Kuramitsu, *Isolation and characterization of a hemin-regulated gene, hemR, from Porphyromonas gingivalis*. J Bacteriol, 1997. **179**(6): p. 1898-908.
37. Kesavalu, L., S.C. Holt, and J.L. Ebersole, *Trypsin-like protease activity of Porphyromonas gingivalis as a potential virulence factor in a murine lesion model*. Microb Pathog, 1996. **20**(1): p. 1-10.
38. Kojima, T., S. Yasui, and I. Ishikawa, *Distribution of Porphyromonas gingivalis in adult periodontitis patients*. J Periodontol, 1993. **64**(12): p. 1231-7.
39. Simonson, L.G., et al., *Quantitative relationship of Treponema denticola to severity of periodontal disease*. Infect Immun, 1988. **56**(4): p. 726-8.
40. Williams, R.C., et al., *Treatment of periodontitis by local administration of minocycline microspheres: a controlled trial*. J Periodontol, 2001. **72**(11): p. 1535-44.

41. Marsh, P.D. and E. Zaura, *Dental biofilm: ecological interactions in health and disease*. J Clin Periodontol, 2017. **44 Suppl 18**: p. S12-S22.
42. Marsh, P.D., *Dental plaque as a biofilm and a microbial community - implications for health and disease*. BMC Oral Health, 2006. **6 Suppl 1**: p. S14.
43. Marsh, P.D., *Dental plaque as a microbial biofilm*. Caries Res, 2004. **38**(3): p. 204-11.
44. Hajishengallis, G. and R.J. Lamont, *Breaking bad: manipulation of the host response by Porphyromonas gingivalis*. Eur J Immunol, 2014. **44**(2): p. 328-38.
45. Hajishengallis, G., *Immunomicrobial pathogenesis of periodontitis: keystones, pathobionts, and host response*. Trends Immunol, 2014. **35**(1): p. 3-11.
46. Hong, B.Y., et al., *Microbiome profiles in periodontitis in relation to host and disease characteristics*. PLoS One, 2015. **10**(5): p. e0127077.
47. Tonetti, M.S., I.L. Chapple, and P. Working Group 3 of Seventh European Workshop on, *Biological approaches to the development of novel periodontal therapies--consensus of the Seventh European Workshop on Periodontology*. J Clin Periodontol, 2011. **38 Suppl 11**: p. 114-8.
48. Sanz, M., et al., *Seventh European Workshop on Periodontology of the European Academy of Periodontology at the Parador at la Granja, Segovia, Spain*. J Clin Periodontol, 2011. **38 Suppl 11**: p. 1-2.
49. Baeza, M., et al., *Diagnostic accuracy for apical and chronic periodontitis biomarkers in gingival crevicular fluid: an exploratory study*. J Clin Periodontol, 2016. **43**(1): p. 34-45.
50. Hajishengallis, G., R.P. Darveau, and M.A. Curtis, *The keystone-pathogen hypothesis*. Nat Rev Microbiol, 2012. **10**(10): p. 717-25.
51. Hajishengallis, G., et al., *Low-abundance biofilm species orchestrates inflammatory periodontal disease through the commensal microbiota and complement*. Cell Host Microbe, 2011. **10**(5): p. 497-506.
52. Darveau, R.P., G. Hajishengallis, and M.A. Curtis, *Porphyromonas gingivalis as a potential community activist for disease*. J Dent Res, 2012. **91**(9): p. 816-20.
53. Doungudomdacha, S., A. Rawlinson, and C.W. Douglas, *Enumeration of Porphyromonas gingivalis, Prevotella intermedia and Actinobacillus actinomycetemcomitans in subgingival plaque samples by a quantitative-competitive PCR method*. J Med Microbiol, 2000. **49**(10): p. 861-74.
54. Kumar, P.S., et al., *Changes in periodontal health status are associated with bacterial community shifts as assessed by quantitative 16S cloning and sequencing*. J Clin Microbiol, 2006. **44**(10): p. 3665-73.
55. Abusleme, L., et al., *The subgingival microbiome in health and periodontitis and its relationship with community biomass and inflammation*. ISME J, 2013. **7**(5): p. 1016-25.
56. Darveau, R.P., *Periodontitis: a polymicrobial disruption of host homeostasis*. Nat Rev Microbiol, 2010. **8**(7): p. 481-90.
57. Berezow, A.B. and R.P. Darveau, *Microbial shift and periodontitis*. Periodontol 2000, 2011. **55**(1): p. 36-47.
58. Zenobia, C. and G. Hajishengallis, *Porphyromonas gingivalis virulence factors involved in subversion of leukocytes and microbial dysbiosis*. Virulence, 2015. **6**(3): p. 236-43.
59. Guo, Y., K.A. Nguyen, and J. Potempa, *Dichotomy of gingipains action as virulence factors: from cleaving substrates with the precision of a surgeon's knife to a meat chopper-like brutal degradation of proteins*. Periodontol 2000, 2010. **54**(1): p. 15-44.

60. Potempa, J., et al., *Gingipains, the major cysteine proteinases and virulence factors of Porphyromonas gingivalis: structure, function and assembly of multidomain protein complexes*. *Curr Protein Pept Sci*, 2003. **4**(6): p. 397-407.
61. Curtis, M.A., et al., *Molecular genetics and nomenclature of proteases of Porphyromonas gingivalis*. *J Periodontal Res*, 1999. **34**(8): p. 464-72.
62. Nguyen, K.A., J. Travis, and J. Potempa, *Does the importance of the C-terminal residues in the maturation of RgpB from Porphyromonas gingivalis reveal a novel mechanism for protein export in a subgroup of Gram-Negative bacteria?* *J Bacteriol*, 2007. **189**(3): p. 833-43.
63. Seers, C.A., et al., *The RgpB C-terminal domain has a role in attachment of RgpB to the outer membrane and belongs to a novel C-terminal-domain family found in Porphyromonas gingivalis*. *J Bacteriol*, 2006. **188**(17): p. 6376-86.
64. Al-Shibani, N. and L.J. Windsor, *Effects of Porphyromonas gingivalis on human gingival fibroblasts from healthy and inflamed tissues*. *J Periodontal Res*, 2008. **43**(4): p. 465-70.
65. Grayson, R., et al., *Activation of human matrix metalloproteinase 2 by gingival crevicular fluid and Porphyromonas gingivalis*. *J Clin Periodontol*, 2003. **30**(6): p. 542-50.
66. DeCarlo, A.A., Jr., et al., *Activation and novel processing of matrix metalloproteinases by a thiol-proteinase from the oral anaerobe Porphyromonas gingivalis*. *J Dent Res*, 1997. **76**(6): p. 1260-70.
67. Groeger, S., et al., *Effects of Porphyromonas gingivalis infection on human gingival epithelial barrier function in vitro*. *Eur J Oral Sci*, 2010. **118**(6): p. 582-9.
68. Bengtsson, T., A. Khalaf, and H. Khalaf, *Secreted gingipains from Porphyromonas gingivalis colonies exert potent immunomodulatory effects on human gingival fibroblasts*. *Microbiol Res*, 2015. **178**: p. 18-26.
69. Facey, S.J. and A. Kuhn, *Biogenesis of bacterial inner-membrane proteins*. *Cell Mol Life Sci*, 2010. **67**(14): p. 2343-62.
70. Pugsley, A.P., *The complete general secretory pathway in gram-negative bacteria*. *Microbiol Rev*, 1993. **57**(1): p. 50-108.
71. Lasica, A.M., et al., *The Type IX Secretion System (T9SS): Highlights and Recent Insights into Its Structure and Function*. *Front Cell Infect Microbiol*, 2017. **7**: p. 215.
72. Abby, S.S., et al., *Identification of protein secretion systems in bacterial genomes*. *Sci Rep*, 2016. **6**: p. 23080.
73. Veith, P.D., et al., *Protein substrates of a novel secretion system are numerous in the Bacteroidetes phylum and have in common a cleavable C-terminal secretion signal, extensive post-translational modification, and cell-surface attachment*. *J Proteome Res*, 2013. **12**(10): p. 4449-61.
74. Auclair, S.M., M.K. Bhanu, and D.A. Kendall, *Signal peptidase I: cleaving the way to mature proteins*. *Protein Sci*, 2012. **21**(1): p. 13-25.
75. Paetzel, M., et al., *Signal peptidases*. *Chem Rev*, 2002. **102**(12): p. 4549-80.
76. von Heijne, G., *Signal sequences. The limits of variation*. *Journal of molecular biology*, 1985. **184**(1): p. 99-105.
77. Sankaran, K. and H.C. Wu, *Lipid modification of bacterial prolipoprotein. Transfer of diacylglycerol moiety from phosphatidylglycerol*. *The Journal of biological chemistry*, 1994. **269**(31): p. 19701-6.
78. Yamagata, H., et al., *Genetic characterization of a gene for prolipoprotein signal peptidase in Escherichia coli*. *Molecular & general genetics : MGG*, 1983. **192**(1-2): p. 10-4.

79. Hayashi, S. and H.C. Wu, *Lipoproteins in bacteria*. Journal of bioenergetics and biomembranes, 1990. **22**(3): p. 451-71.
80. Okuda, S. and H. Tokuda, *Lipoprotein sorting in bacteria*. Annu Rev Microbiol, 2011. **65**: p. 239-59.
81. Seifert, F., et al., *Phosphate ions and glutaminy cyclases catalyze the cyclization of glutaminy residues by facilitating synchronized proton transfers*. Bioorganic chemistry, 2015. **60**: p. 98-101.
82. Seifert, F., et al., *Glutaminy cyclases display significant catalytic proficiency for glutamyl substrates*. Biochemistry, 2009. **48**(50): p. 11831-3.
83. Stephan, A., et al., *Mammalian glutaminy cyclases and their isoenzymes have identical enzymatic characteristics*. FEBS J, 2009. **276**(22): p. 6522-36.
84. Adamson, S.W., et al., *Molecular characterization of tick salivary gland glutaminy cyclase*. Insect Biochem Mol Biol, 2013. **43**(9): p. 781-93.
85. Schmir, G.L., *The Effect of Structural Variation on the Hydrolysis of Delta-2-Thiazolines*. J Am Chem Soc, 1965. **87**: p. 2743-51.
86. Meyer, D., et al., *Unexpected tautomeric equilibria of the carbanion-enamine intermediate in pyruvate oxidase highlight unrecognized chemical versatility of thiamin*. Proc Natl Acad Sci U S A, 2012. **109**(27): p. 10867-72.
87. Sobolewski, A.L., W. Domcke, and C. Hattig, *Tautomeric selectivity of the excited-state lifetime of guanine/cytosine base pairs: the role of electron-driven proton-transfer processes*. Proc Natl Acad Sci U S A, 2005. **102**(50): p. 17903-6.
88. Huang, K.-F., et al., *A conserved hydrogen-bond network in the catalytic centre of animal glutaminy cyclases is critical for catalysis*. Biochemical Journal, 2008. **411**(1): p. 181-190.
89. Seifert, F., et al., *Phosphate ions and glutaminy cyclases catalyze the cyclization of glutaminy residues by facilitating synchronized proton transfers*. Bioorg Chem, 2015. **60**: p. 98-101.
90. Messer, M. and M. Ottesen, *Isolation and properties of glutamine cyclotransferase of dried papaya latex*. C R Trav Lab Carlsberg, 1965. **35**(1): p. 1-24.
91. Huang, W.L., et al., *Crystal structure and functional analysis of the glutaminy cyclase from Xanthomonas campestris*. J Mol Biol, 2010. **401**(3): p. 374-88.
92. Schilling, S., et al., *Isolation, catalytic properties, and competitive inhibitors of the zinc-dependent murine glutaminy cyclase*. Biochemistry, 2005. **44**(40): p. 13415-24.
93. Schilling, S., et al., *Isolation and characterization of glutaminy cyclases from Drosophila: evidence for enzyme forms with different subcellular localization*. Biochemistry, 2007. **46**(38): p. 10921-30.
94. Schilling, S., et al., *Identification of human glutaminy cyclase as a metalloenzyme. Potent inhibition by imidazole derivatives and heterocyclic chelators*. J Biol Chem, 2003. **278**(50): p. 49773-9.
95. Richter, K., et al., *Biosynthesis of thyrotropin releasing hormone in the skin of Xenopus laevis: partial sequence of the precursor deduced from cloned cDNA*. EMBO J, 1984. **3**(3): p. 617-21.
96. Aii, K., et al., *Degradation kinetics of L-glutamine in aqueous solution*. Eur J Pharm Sci, 1999. **9**(1): p. 75-8.
97. Messer, M. and M. Ottesen, *Isolation and Properties of Glutamine Cyclotransferase of Dried Papaya Latex*. Biochim Biophys Acta, 1964. **92**: p. 409-11.
98. Messer, M., *Enzymatic cyclization of L-glutamine and L-glutaminy peptides*. Nature, 1963. **197**: p. 1299.

99. Busby, W.H., Jr., et al., *An enzyme(s) that converts glutaminy-peptides into pyroglutamyl-peptides. Presence in pituitary, brain, adrenal medulla, and lymphocytes.* J Biol Chem, 1987. **262**(18): p. 8532-6.
100. Dahl, S.W., et al., *Carica papaya glutamine cyclotransferase belongs to a novel plant enzyme subfamily: cloning and characterization of the recombinant enzyme.* Protein Expr Purif, 2000. **20**(1): p. 27-36.
101. Fischer, W.H. and J. Spiess, *Identification of a mammalian glutaminy cyclase converting glutaminy into pyroglutamyl peptides.* Proc Natl Acad Sci U S A, 1987. **84**(11): p. 3628-32.
102. Pohl, T., et al., *Primary structure and functional expression of a glutaminy cyclase.* Proc Natl Acad Sci U S A, 1991. **88**(22): p. 10059-63.
103. Zerhouni, S., et al., *Purification and characterization of papaya glutamine cyclotransferase, a plant enzyme highly resistant to chemical, acid and thermal denaturation.* Biochim Biophys Acta, 1998. **1387**(1-2): p. 275-90.
104. Wintjens, R., et al., *Crystal structure of papaya glutaminy cyclase, an archetype for plant and bacterial glutaminy cyclases.* Journal of molecular biology, 2006. **357**(2): p. 457-70.
105. Russell, R.B., P.D. Sasieni, and M.J. Sternberg, *Supersites within superfolds. Binding site similarity in the absence of homology.* J Mol Biol, 1998. **282**(4): p. 903-18.
106. Oberg, K.A., et al., *Papaya glutamine cyclase, a plant enzyme highly resistant to proteolysis, adopts an all-beta conformation.* Eur J Biochem, 1998. **258**(1): p. 214-22.
107. Bateman, R.C., Jr., et al., *Evidence for essential histidines in human pituitary glutaminy cyclase.* Biochemistry, 2001. **40**(37): p. 11246-50.
108. Schilling, S., et al., *Heterologous expression and characterization of human glutaminy cyclase: evidence for a disulfide bond with importance for catalytic activity.* Biochemistry, 2002. **41**(35): p. 10849-57.
109. Van Coillie, E., et al., *Functional comparison of two human monocyte chemotactic protein-2 isoforms, role of the amino-terminal pyroglutamic acid and processing by CD26/dipeptidyl peptidase IV.* Biochemistry, 1998. **37**(36): p. 12672-80.
110. Hinke, S.A., et al., *Dipeptidyl peptidase IV (DPIV/CD26) degradation of glucagon. Characterization of glucagon degradation products and DPIV-resistant analogs.* J Biol Chem, 2000. **275**(6): p. 3827-34.
111. Jawhar, S., O. Wirths, and T.A. Bayer, *Pyroglutamate amyloid-beta (Abeta): a hatchet man in Alzheimer disease.* J Biol Chem, 2011. **286**(45): p. 38825-32.
112. Huang, K.F., et al., *A conserved hydrogen-bond network in the catalytic centre of animal glutaminy cyclases is critical for catalysis.* Biochem J, 2008. **411**(1): p. 181-90.
113. Huang, K.F., et al., *Crystal structures of human glutaminy cyclase, an enzyme responsible for protein N-terminal pyroglutamate formation.* Proc Natl Acad Sci U S A, 2005. **102**(37): p. 13117-22.
114. Buchholz, M., et al., *Inhibitors for human glutaminy cyclase by structure based design and bioisosteric replacement.* J Med Chem, 2009. **52**(22): p. 7069-80.
115. Wang, Y.M., K.F. Huang, and I.H. Tsai, *Snake venom glutaminy cyclases: purification, cloning, kinetic study, recombinant expression, and comparison with the human enzyme.* Toxicon, 2014. **86**: p. 40-50.
116. Ferreira, S.H. and M. Rocha e Silva, *Potentiation of bradykinin and eledoisin by BPF (bradykinin potentiating factor) from Bothrops jararaca venom.* Experientia, 1965. **21**(6): p. 347-9.

117. Murayama, N., et al., *Cloning and sequence analysis of a Bothrops jararaca cDNA encoding a precursor of seven bradykinin-potentiating peptides and a C-type natriuretic peptide*. Proc Natl Acad Sci U S A, 1997. **94**(4): p. 1189-93.
118. Wagstaff, S.C., et al., *Molecular characterisation of endogenous snake venom metalloproteinase inhibitors*. Biochem Biophys Res Commun, 2008. **365**(4): p. 650-6.
119. Huang, K.F., et al., *Determinants of the inhibition of a Taiwan habu venom metalloproteinase by its endogenous inhibitors revealed by X-ray crystallography and synthetic inhibitor analogues*. Eur J Biochem, 2002. **269**(12): p. 3047-56.
120. Booth, R.E., et al., *Human glutaminyl cyclase and bacterial zinc aminopeptidase share a common fold and active site*. BMC Biol, 2004. **2**: p. 2.
121. Huang, K.F., Y.L. Liu, and A.H. Wang, *Cloning, expression, characterization, and crystallization of a glutaminyl cyclase from human bone marrow: a single zinc metalloenzyme*. Protein Expr Purif, 2005. **43**(1): p. 65-72.
122. Gololobov, M.Y., W. Wang, and R.C. Bateman, Jr., *Substrate and inhibitor specificity of glutamine cyclotransferase (QC)*. Biol Chem Hoppe Seyler, 1996. **377**(6): p. 395-8.
123. Schilling, S., et al., *Substrate specificity of glutaminyl cyclases from plants and animals*. Biol Chem, 2003. **384**(12): p. 1583-92.
124. Bockers, T.M., M.R. Kreutz, and T. Pohl, *Glutaminyl-cyclase expression in the bovine/porcine hypothalamus and pituitary*. J Neuroendocrinol, 1995. **7**(6): p. 445-53.
125. Song, I., C.Z. Chuang, and R.C. Bateman, Jr., *Molecular cloning, sequence analysis and expression of human pituitary glutaminyl cyclase*. J Mol Endocrinol, 1994. **13**(1): p. 77-86.
126. Azarkan, M., et al., *Crystallization and preliminary X-ray diffraction studies of the glutaminyl cyclase from Carica papaya latex*. Acta Crystallogr Sect F Struct Biol Cryst Commun, 2005. **61**(Pt 1): p. 59-61.
127. Azarkan, M., et al., *Detection of three wound-induced proteins in papaya latex*. Phytochemistry, 2004. **65**(5): p. 525-34.
128. Schilling, S., et al., *Continuous spectrometric assays for glutaminyl cyclase activity*. Anal Biochem, 2002. **303**(1): p. 49-56.
129. Buchholz, M., et al., *The first potent inhibitors for human glutaminyl cyclase: synthesis and structure-activity relationship*. J Med Chem, 2006. **49**(2): p. 664-77.
130. Sato, K., et al., *Identification of Porphyromonas gingivalis proteins secreted by the Por secretion system*. FEMS Microbiol Lett, 2013. **338**(1): p. 68-76.
131. Sato, K., et al., *A protein secretion system linked to bacteroidete gliding motility and pathogenesis*. Proc Natl Acad Sci U S A, 2010. **107**(1): p. 276-81.
132. McBride, M.J. and Y. Zhu, *Gliding motility and Por secretion system genes are widespread among members of the phylum bacteroidetes*. J Bacteriol, 2013. **195**(2): p. 270-8.
133. de Diego, I., et al., *The outer-membrane export signal of Porphyromonas gingivalis type IX secretion system (T9SS) is a conserved C-terminal beta-sandwich domain*. Sci Rep, 2016. **6**: p. 23123.
134. Veith, P.D., et al., *Major outer membrane proteins and proteolytic processing of RgpA and Kgp of Porphyromonas gingivalis W50*. Biochem J, 2002. **363**(Pt 1): p. 105-15.
135. Veith, P.D., et al., *Outer membrane proteome and antigens of Tannerella forsythia*. J Proteome Res, 2009. **8**(9): p. 4279-92.

136. Veith, P.D., et al., *Porphyromonas gingivalis* outer membrane vesicles exclusively contain outer membrane and periplasmic proteins and carry a cargo enriched with virulence factors. *J Proteome Res*, 2014. **13**(5): p. 2420-32.
137. Veith, P.D., et al., *Tannerella forsythia* Outer Membrane Vesicles Are Enriched with Substrates of the Type IX Secretion System and TonB-Dependent Receptors. *J Proteome Res*, 2015. **14**(12): p. 5355-66.
138. TheUniProtConsortium, *UniProt: the universal protein knowledgebase*. *Nucleic acids research*, 2017. **45**(D1): p. D158-D169.
139. Petersen, T.N., et al., *SignalP 4.0: discriminating signal peptides from transmembrane regions*. *Nature methods*, 2011. **8**(10): p. 785-6.
140. Juncker, A.S., et al., *Prediction of lipoprotein signal peptides in Gram-negative bacteria*. *Protein science : a publication of the Protein Society*, 2003. **12**(8): p. 1652-62.
141. Crooks, G.E., et al., *WebLogo: a sequence logo generator*. *Genome research*, 2004. **14**(6): p. 1188-90.
142. Nguyen, K.A., et al., *Verification of a topology model of PorT as an integral outer-membrane protein in Porphyromonas gingivalis*. *Microbiology*, 2009. **155**(Pt 2): p. 328-37.
143. Lasica, A.M., et al., *Structural and functional probing of PorZ, an essential bacterial surface component of the type-IX secretion system of human oral-microbiomic Porphyromonas gingivalis*. *Sci Rep*, 2016. **6**: p. 37708.
144. Gibson, D.G., et al., *Enzymatic assembly of DNA molecules up to several hundred kilobases*. *Nat Methods*, 2009. **6**(5): p. 343-5.
145. Chiu, J., et al., *Site-directed, Ligase-Independent Mutagenesis (SLIM): a single-tube methodology approaching 100% efficiency in 4 h*. *Nucleic Acids Res*, 2004. **32**(21): p. e174.
146. Belanger, M., P. Rodrigues, and A. Progulske-Fox, *Genetic manipulation of Porphyromonas gingivalis*. *Curr Protoc Microbiol*, 2007. **Chapter 13**: p. Unit13C 2.
147. Yu, C.S., C.J. Lin, and J.K. Hwang, *Predicting subcellular localization of proteins for Gram-negative bacteria by support vector machines based on n-peptide compositions*. *Protein Sci*, 2004. **13**(5): p. 1402-6.
148. Schwechheimer, C. and M.J. Kuehn, *Outer-membrane vesicles from Gram-negative bacteria: biogenesis and functions*. *Nat Rev Microbiol*, 2015. **13**(10): p. 605-19.
149. Pathirana, R.D., et al., *Characterization of proteinase-adhesin complexes of Porphyromonas gingivalis*. *Microbiology*, 2006. **152**(Pt 8): p. 2381-94.
150. Woese, C.R., *Bacterial evolution*. *Microbiol Rev*, 1987. **51**(2): p. 221-71.
151. Makarova, K.S., et al., *A putative RNA-interference-based immune system in prokaryotes: computational analysis of the predicted enzymatic machinery, functional analogies with eukaryotic RNAi, and hypothetical mechanisms of action*. *Biol Direct*, 2006. **1**: p. 7.
152. Chen, T., et al., *Comparative whole-genome analysis of virulent and avirulent strains of Porphyromonas gingivalis*. *J Bacteriol*, 2004. **186**(16): p. 5473-9.
153. Tenorio, E.L., et al., *Identification of interspecies interactions affecting Porphyromonas gingivalis virulence phenotypes*. *J Oral Microbiol*, 2011. **3**.

CURRICULUM VITA

NAME: John Andrew Houston

EDUCATION AND TRAINING:

Graduate of Columbia Central High School (2004) Columbia, TN

Samford University, (2004-2008) Birmingham, AL

- Bachelors Degree in Biology

University of Louisville, Louisville, KY

- DMD/Ph.D. combined program student

POSTERS:

Porphyromonas gingivalis Glutaminyl Cylcase resembles a Human Enzyme and constitutes a novel target for treatment of Periodontal Disease.

- Research! Louisville 2011, Hinman Student Research Symposium 2011

Cyclization of the N-terminal Gln residue in proteins secreted by *Porphyromonas gingivalis* is essential for normal secretion and processing of gingipains.

- Research! Louisville 2012

Inhibition of *Porphyromonas gingivalis* glutaminyl cyclase blocks growth of the bacteria

- Research! Louisville 2014

Awards and Scholarships

Most Outstanding Presentation in Basic Science – Hinman Student Research Symposium 2011

DMD/Ph.D. Scholarship – University of Louisville School of Dentistry 2012-present

Research! Louisville 1st Place Basic Science Poster 2014

Edward & Mary Smith Scholarship 2013-2014

Pierre Fauchard Academy Dental School Scholarship 2016

PUBLICATIONS:

[Purification and characterisation of recombinant His-tagged RgpB gingipain from Porphyromonas gingivalis.](#) Veillard F, Potempa B, Guo Y, Ksiazek M, Sztukowska MN, Houston JA, Koneru L, Nguyen KA, Potempa J. Biol Chem. 2015

[Inhibition of gingipains by their profragments as the mechanism protecting Porphyromonas gingivalis against premature activation of secreted proteases.](#) Veillard F, Sztukowska M, Mizgalska D, Ksiazek M, Houston J, Potempa B, Enghild JJ, Thøgersen IB, Gomis-Rüth FX, Nguyen KA, Potempa J. Biochim Biophys Acta. 2013

The outer-membrane export signal of Porphyromonas gingivalis type IX secretion system (T9SS) is a conserved C-terminal β -sandwich domainñaki de Diego Martinez, Miroslaw Ksiazek, Danuta Mizgalska, Lahari Koneru, Przemyslaw Golik, Borys Szmigielski, Magdalena Nowak, Zuzanna Nowakowska, Barbara Potempa, John A. Houston, Jan J. Enghild, Ida B. Thøgersen, Jinlong Gao, Ann H. Kwan, Jill Trewhella, Grzegorz Dubin, F. Xavier Gomis-Rüth, Ky-Anh Nguyen, and Jan Potempa. Sci Rep 2016